Silicon Photomultiplier
- characteristics and applications -

Nicoleta Dinu

Laboratoire de l' Accélérateur Linéaire, IN2P3, CNRS, Orsay, France
Actually with ARTEMIS, CNRS & Observatoire Cote d'Azur, Nice, France

Seminar at IIHE, Brussels, 04.03.2016

OUTLINE

- PART A:
  - Silicon Photomultiplier (SiPM)
    - Short review of SiPM precursors: PIN, APD, GM-APD
    - SiPM design and physics principle
    - SiPM electrical and optical characteristics
- PART B:
  - SiPM applications
    - Medical imaging: compact imaging gamma camera
    - How to select the most adapted SiPM for a given application??

PART A:

Silicon Photomultiplier

Review of SiPM precursors (I)

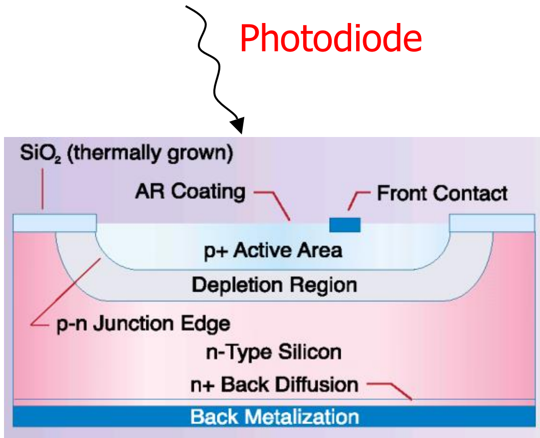

p-n junction,
reversed V_{bias} – 0-3 V

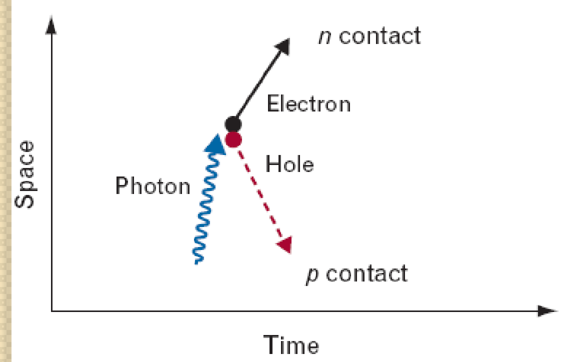

Gain = 1

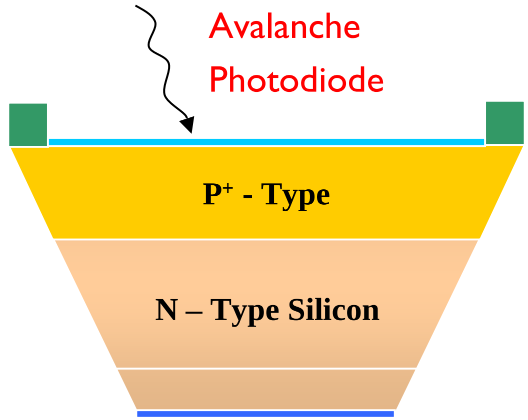

p-n junction,
reversed $V_{bias} < V_{BD}$

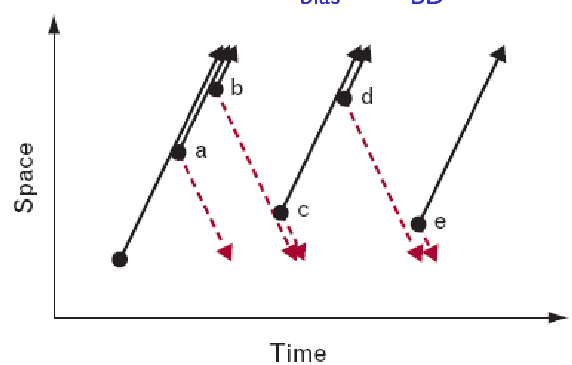

Gain = M (~ 50-500)

- linear mode operation-

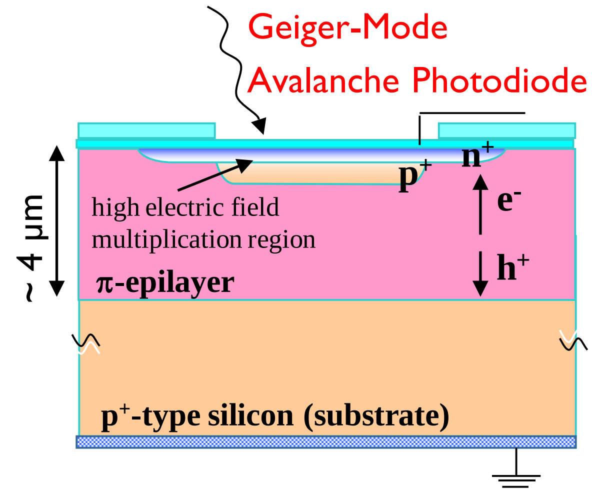

p-n junction,
reversed $V_{bias} > V_{BD}$

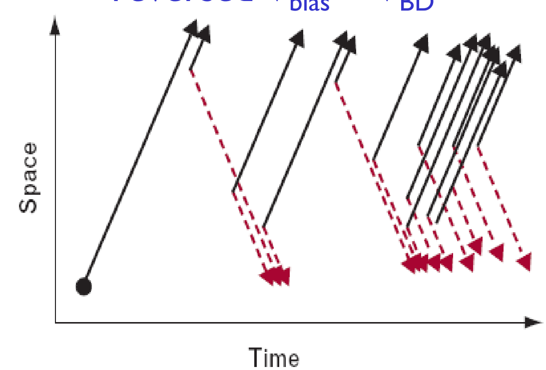

Gain → infinite

-Geiger-mode operation-

Review of SiPM precursors (2)

- p-n junction working in reverse bias mode

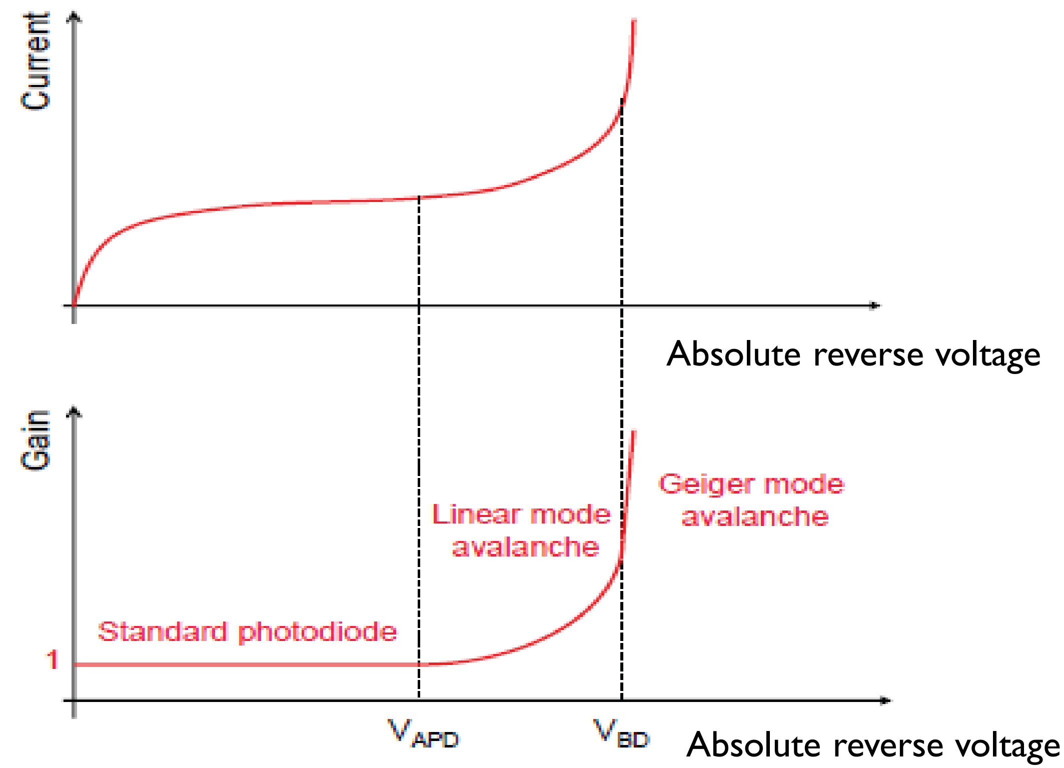

Photodiode

- $0 < V_{bias} < V_{APD}$ (few volts)
- G = 1
- Operate at high light level (few hundreds of photons)

APD

- $V_{APD} < V_{bias} < V_{BD}$
- G = M (50 - 500)
- Linear-mode operation
- Operate at medium light level (tens of photons)

GM-APD or SPAD

- $V_{bias} > V_{BD}$ (V_{bias}-V_{BD} ~ few volts)
- G ⇨ ∞
- Geiger-mode operation
- Can operate at single photon level

Geiger-Mode Avalanche Photodiode

The first single photon detectors operated in Geiger-mode

Planar structure ("thin")

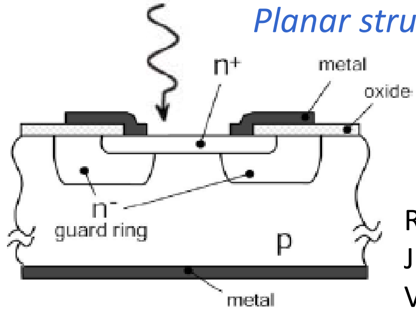

R.H. Haitz
J. Appl. Phys.,
Vol. 36, No. 10 (1965) 3123

Reach-through structure ("thick")

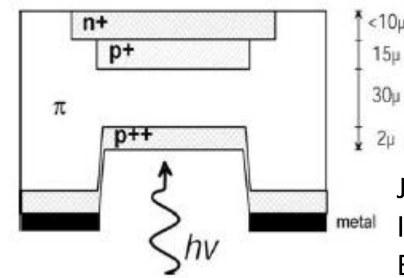

J.R. McIntire
IEEE Trans. Elec. Dev.
ED-13 (1966) 164

Avalanche process in silicon: studied more than 50 years and widely exploited, but not yet understood in details

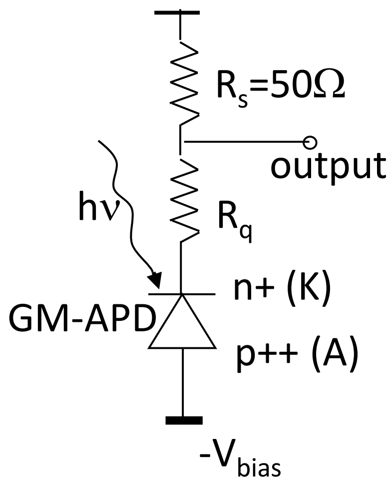

Passive quenching/reset circuit

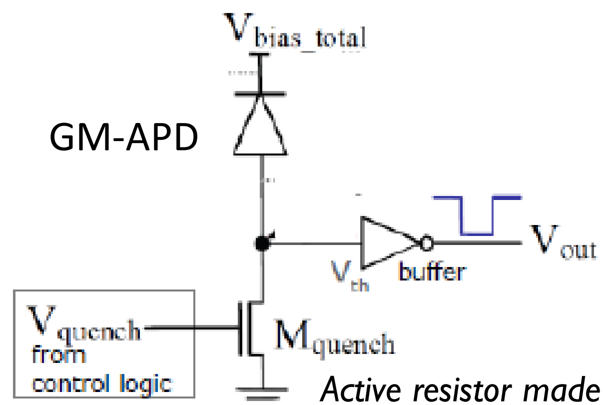

Active resistor made of MOS transistor controlled by a fast electronics

Active quenching/reset circuit

S. Cova & al., Appl. Opt., Vol. 35, No 12 (1996) 1956

SiPM μcell – design and physics principle

- GM-APD (p-n junction) connected in series with quenching resistance R_Q
- GM-APD and R_Q – on the same substrate

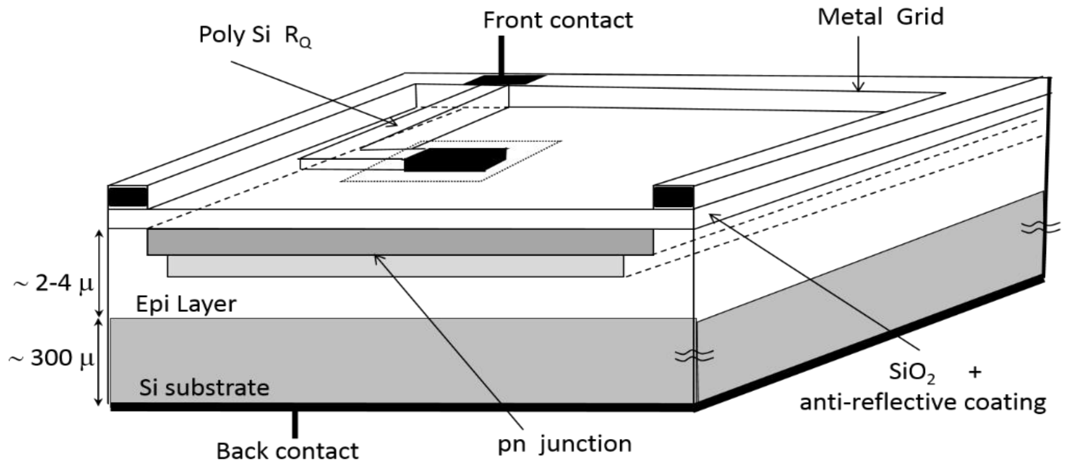

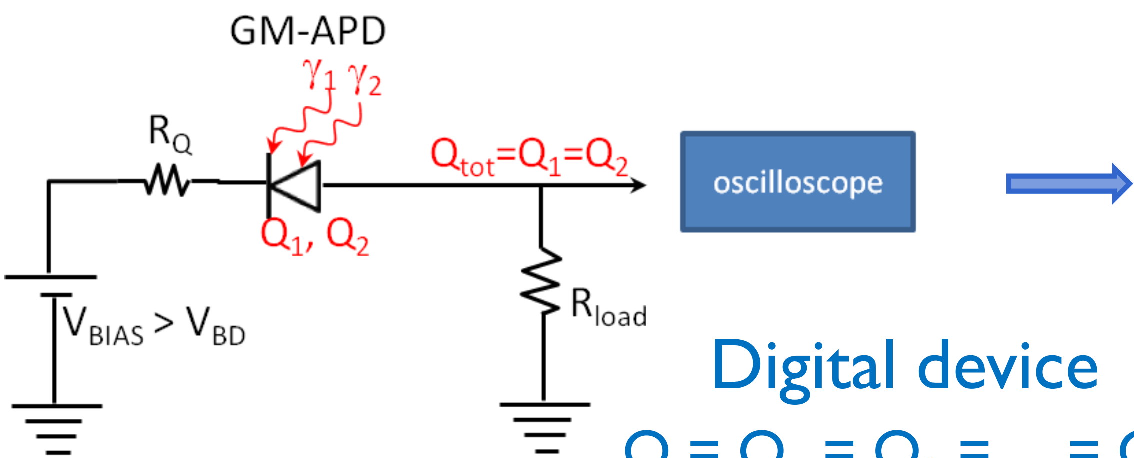

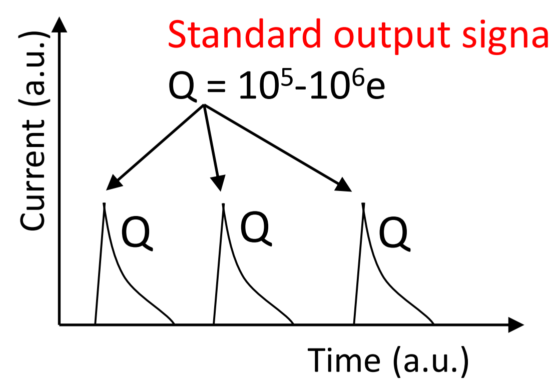

Digital device

$Q = Q_1 = Q_2 = \ldots = Q_n$

No information on light intensity

SiPM – design and physics principle

- Parallel array of μ-cells on the same substrate
  - Each μ-cell: GM-APD in series with R_Q

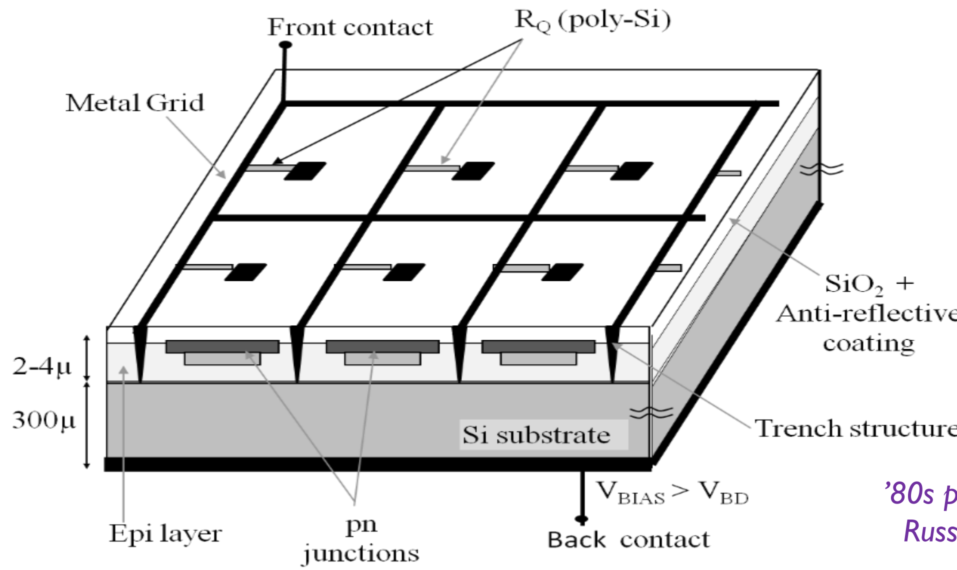

'80s proposed by V.M. Golovin & Z. Sadygov, Russian patents

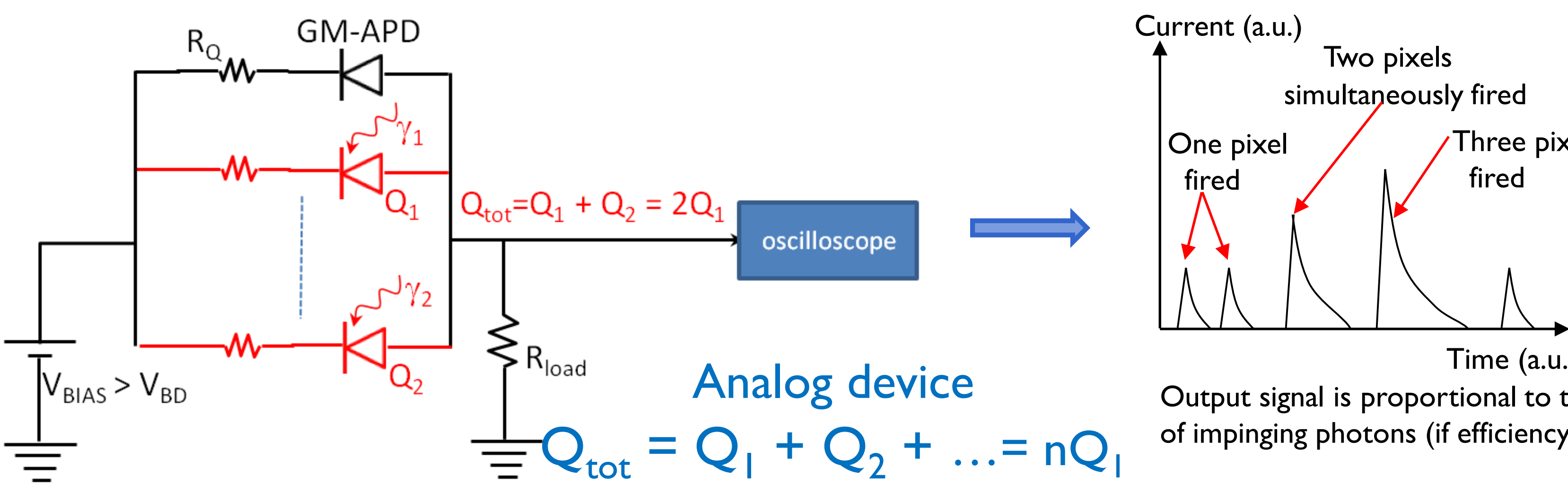

Analog device

$$Q_{tot} = Q_1 + Q_2 + \ldots = nQ_1$$

Output signal is proportional to the nr. of impinging photons (if efficiency = 1)

Many SiPM producers over the world

From W. Ootani, CERN, 2015

- SiPM sensors first commercially available in 2006
  - B. Dolgoshein: "An advanced study of silicon photomultiplier", ICFA Bulletin, 2001
  - C. Jackson, "Geiger-mode Avalanche Photodiodes", PhD Thesis, actually chief technology officer at SensL
  - N. Dinu, C. Piemonte & al.: "Development of the first prototypes of SiPM at ITC-irst", Frontiers detectors for frontier physics, Elba, Italy, 2006
- Many research laboratories over the world contributed to this development
  - Interaction between producers and users was very productive

Single SiPM – few examples of design & packages

Hamamatsu HPK (http://jp.hamamatsu.com/)

10x10, 15x15 , 25x25, 50x50, 100x100μm² μcell

wire bonding

1x1mm²

3x3mm²

TSV technology

2x2mm² 3x3mm² 6x6mm²

SensL (http://sensl.com/)

20x20, 35x35, 50x50, 100x100μm² μcell

1x1, 3x3, 6x6 mm²

TSV technology

3x3 & 6x6 mm²

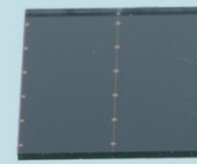

FBK-irst (http://advansid.com/home)

15x15, 40x40, 50x50μm² pixel size

1x1mm²

2x2mm²

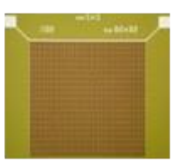

3x3mm²

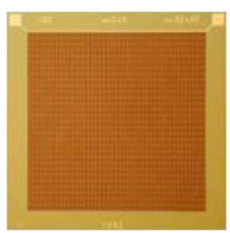

4x4mm²

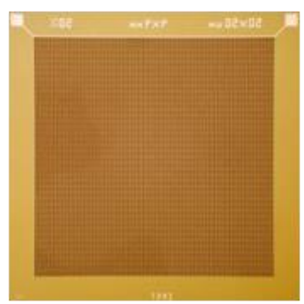

KETEK (http://www.ketek.net/)

25x25, 50x50, 100x100μm² μcell size

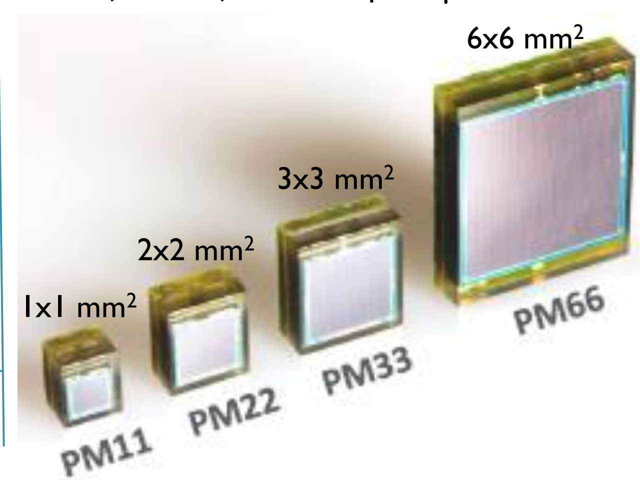

- *Different producers give different names:*
  - *SiPM, MRS-APD, SPM, MPPC…*

Arrays of SiPM – few examples of design & packages

Monolithic arrays
- ☺ small dead area
- ☹ reduced yield

Hamamatsu HPK
Surface mount, ceramic & wire bonding

4(1x4) ch
SiPM: 1x1mm^2
2.45x4.85 mm^2
(~66% dead area)

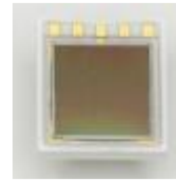

4(2x2) ch
SiPM: 3x3mm^2
9x8.2 mm^2
(~50% dead area)

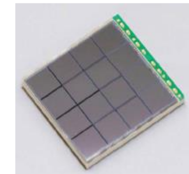

16(4x4) ch
SiPM: 3x3mm^2
13.6x14.3 mm^2
(25% dead area)

FBK-IRST
Surface mount & wire bonding

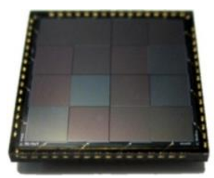

16(4x4) ch
SiPM: 3x3mm^2

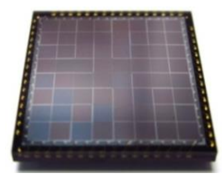

64(8x8) ch
SiPM: 1.5x1.5mm^2

KETEK & HPK (custom devices)
Surface mount & wire bonding

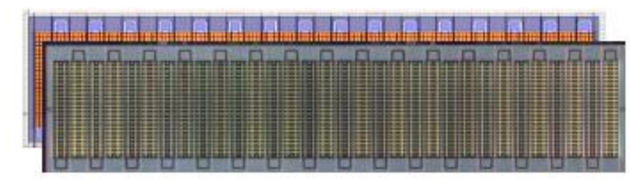

32, 64 or 128 SiPM channels
1 SiPM: 0.25x1.5 mm^2 (LHCb silicon tracker)

Discrete arrays
- ☺ smaller dead area
  - TSV technology
- ☺ high yield
  - select & sort devices

SensL
Surface mount wire bonding & TSV

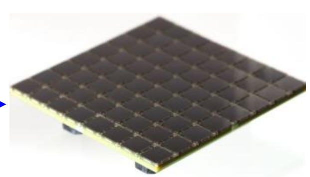

64(8x8) ch
SiPM: 3x3mm^2
29.4x 29.4 mm^2
~ 8 cm^2
(33% dead area)

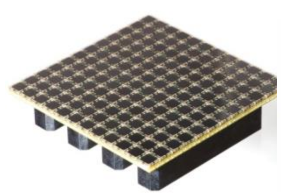

144(12x12) ch
SiPM: 3x3mm^2
43.8x 43.8 mm^2
~ 20 cm^2
(32% dead area)

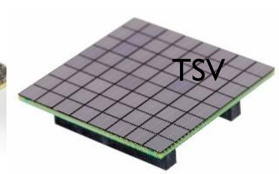

64(8x8) ch
SiPM: 3x3mm^2
24.8x 24.8 mm^2
(7% dead area)

Hamamatsu HPK
Surface mount & TSV

16(4x4) ch
SiPM: 3x3mm^2
12.8x 12.8 mm^2
(12% dead area)

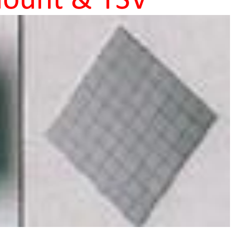

64(8x8) ch
SiPM: 3x3mm^2
24.8x 24.8 mm^2
(7% dead area)

SiPM characteristics from user/application point of view

- Device parameters
  - Photon detection efficiency
  - Signal shape
    - Timing resolution
    - Count rate (linearity)
  - Gain
  - Dark count rate
    - Thermal rate
    - Afterpulses, cross-talk
  - Temperature dependence of various parameters

- System performance
  - Breakdown voltage & operating bias
  - Breakdown uniformity and temperature dependence

Photon detection efficiency

$$PDE = N_{pulses} / N_{photons} = QE \cdot P_{Geiger} \cdot \varepsilon_{geom}$$

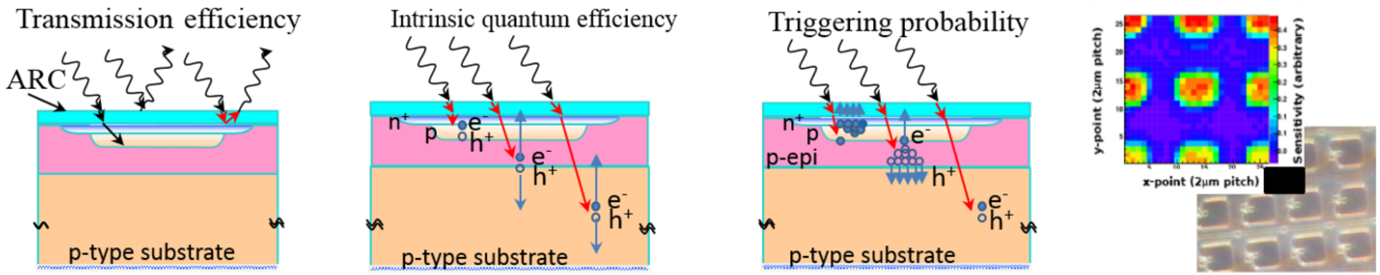

Quantum efficiency (QE)

Avalanche triggering probability (P_{Geiger})

Geometrical fill factor (FF, ε_{geom})

QE of a µcell

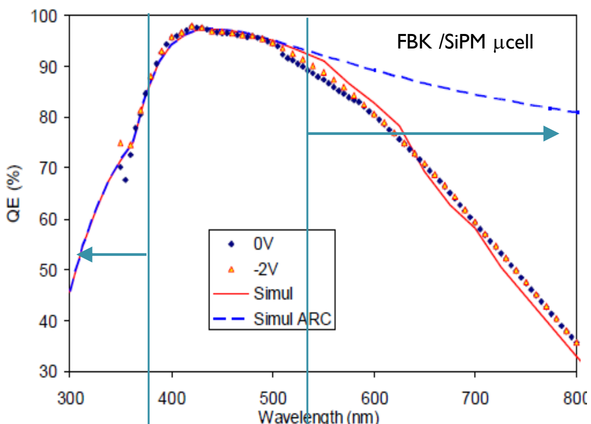

Limited by ARC transmittance & superficial recombination

Limited by small π layer thickness

SiPM / FBK (n-on-p junction)

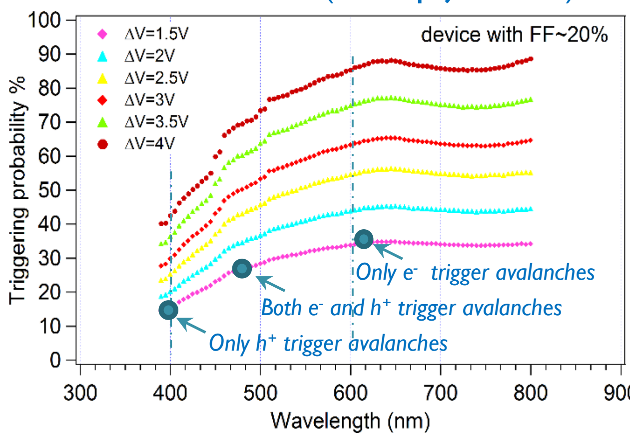

PDE

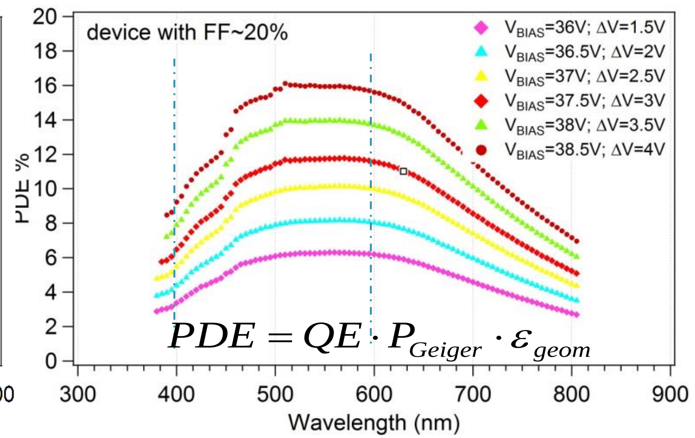

$$PDE = QE \cdot P_{Geiger} \cdot \varepsilon_{geom}$$

Ionization rate in Silicon

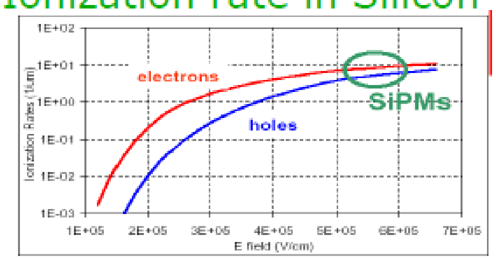

Photon absorbtion length in silicon

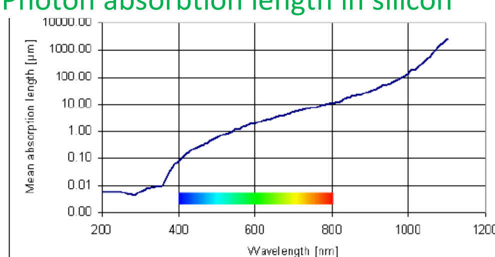

Parameters dependence of PDE

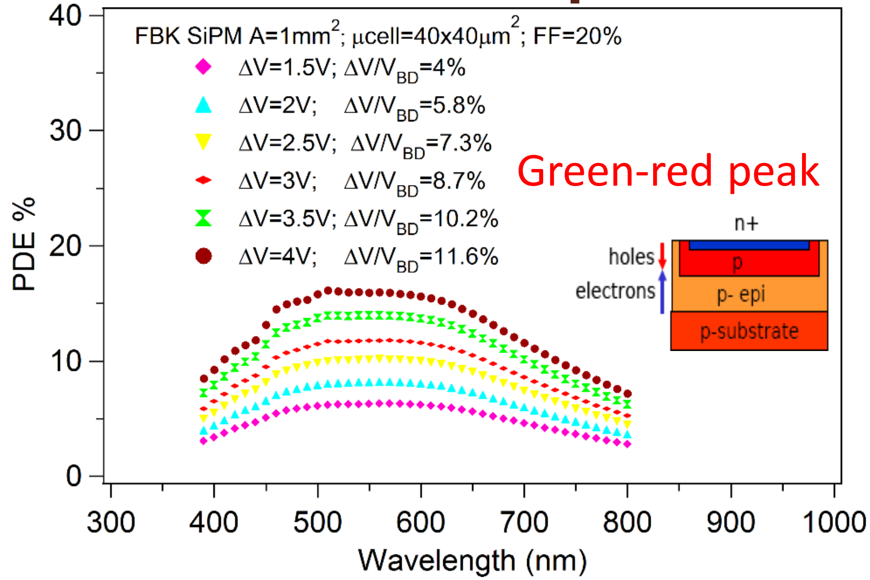

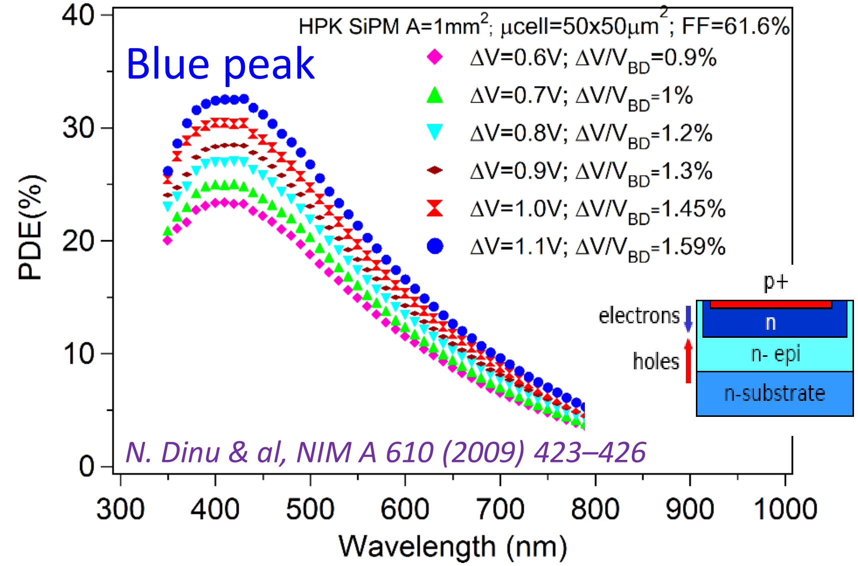

Main absolute scale difference due to fill factor

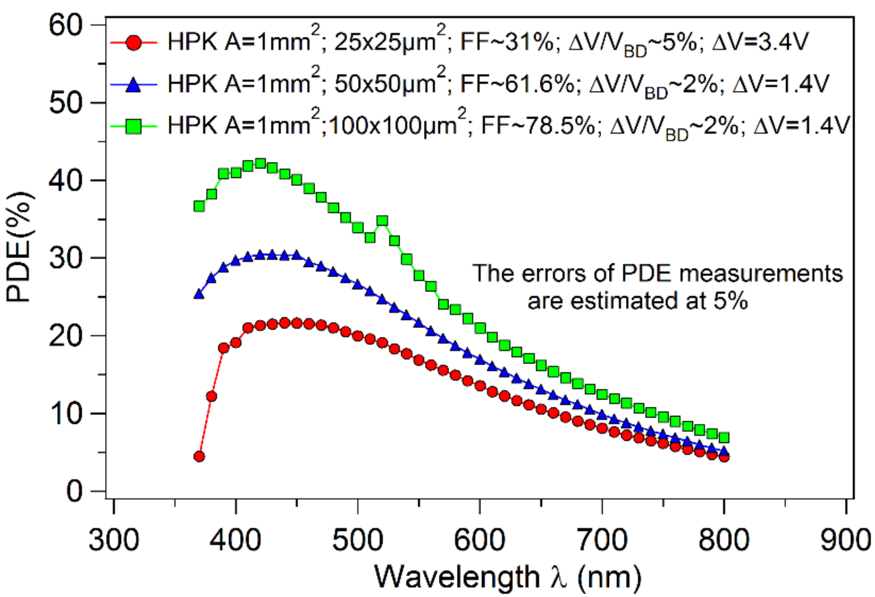

- **PDE depends on:**
  - Light wavelength
    - Junction μcell type
    - p+/n μcell: blue peak ($P_e > P_h$)
    - n+/p μcell : green/red peak
    - peak sensitivity improving
  - Overvoltage
    - increases with ΔV
  - μcell size
    - increases with cell size (ε_{geom} increases)
  - Temperature
    - E_{gap}, mobility, P_{Geiger}
    - more experimental data are required for final modeling

Examples of PDE recent improvements

FBK

High-Density technology in NUV

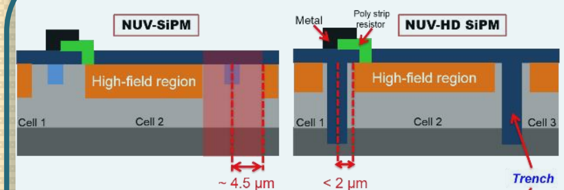

NUV High-Density (HD) technology:
Lower dead border region → Higher Fill Factor
Trenches between cells → Lower Cross-Talk

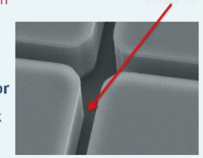

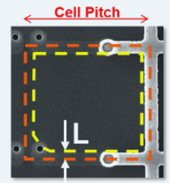

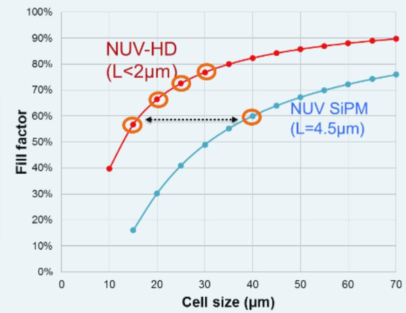

The HD 15 µm pitch is equivalent to the standard 40 µm

T ~25°C, 1x1mm² SiPM, 30µm Cell Pitch, 10V overvoltage

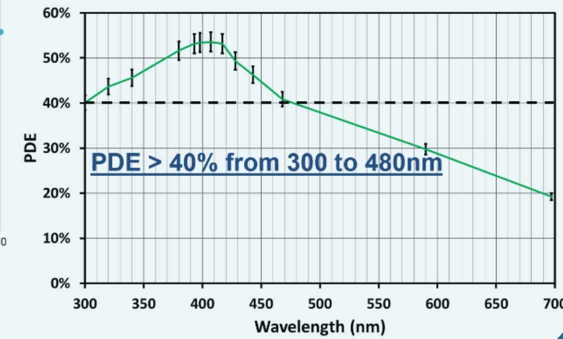

From Zappala & al., VCI, 2016

HPK

MPPC's PDE: direct detection of VUV (LAr's 128nm and LXe's 175nm)

- Our solution for direct detection is the "VUV-MPPC" series.

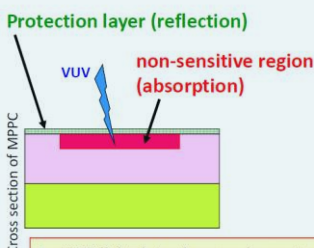

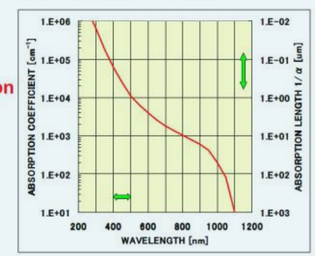

For VUV light detection, precise control of MPPC's protection layer and non-sensitive region is required.

PDE of VUV3 MPPC - 3mm chip w/ 50um pixels

Under vacuum <200nm | In Air >200nm | Gain =1.25x10^6

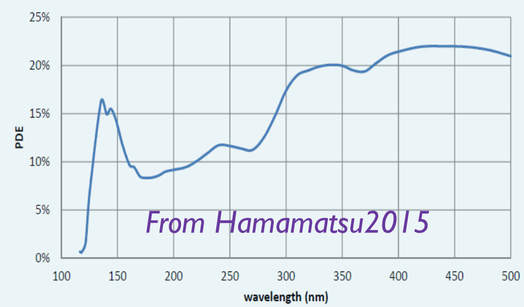

From Hamamatsu2015

Hamamatsu
VUV-enhanced MPPC

→ removal of protection coating
→ optimization of the parameters
- thinner junction
- optimized superficial layers

…

New windows for applications in fundamental Physics experiments
- Dark matter detection
- ν-less double beta decays
- Rare decay modes (MEG)

MPPC Noise (Cross-talk & After-pulsing) Suppression

- After-pulsing suppression
  - Ultralow-defect wafer

- Cross-talk suppression
  - Optical trench around each µcell

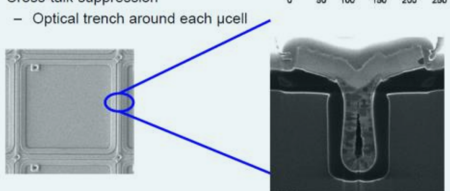

- MPPC (w/ noise suppression) has remarkable PDE @ 420nm!
- For comparison with PMT, please note that PDE = QE x CE

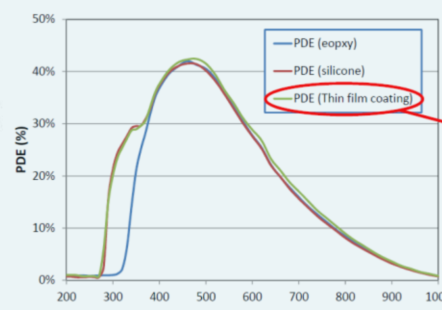

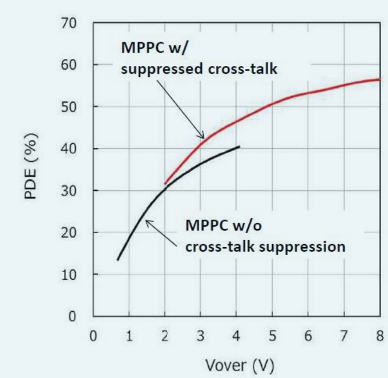

SiPM pulse shape

- Close related to μcell operation and its equivalent circuit
  - Avalanche processes in semiconductors are studied in details since ‘60 for modeling micro-plasma instabilities
  - McIntyre JAP 32 (1961), McIntire IEEE TED (1973, Haitz JAP 35 (1964) and Ruegg IEEE TED 14 (1967)
- SiPM μcell equivalent circuit using simplified Haitz model:
  - GM-APD diode in series with R_Q
  - GM-APD diode
    - capacitance C_D and its series resistance R_D
    - V_{BD} source simulates the breakdown point
    - Switch S : OFF denotes pre-avalanche state ($V_{bias} > V_{BD}$) but no avalanche takes place

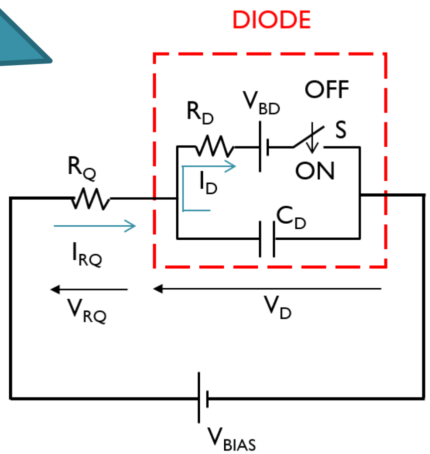

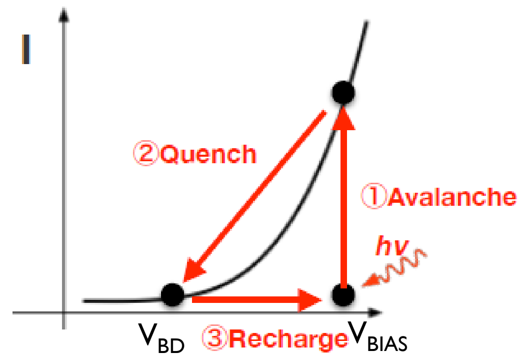

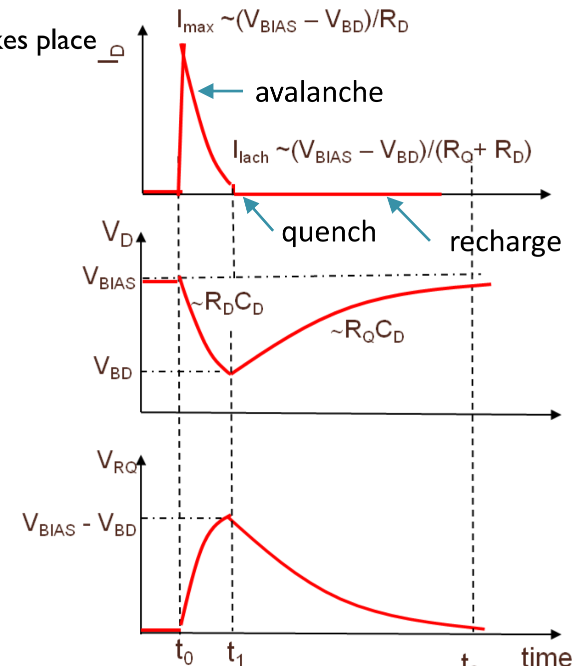

- Operation cycle:

1. Avalanche triggered by a carrier traversing the high field region (switch closed) → short current spike (10^{-11} s) with I_{D_max} ~ $(V_{BIAS}-V_{BD})/R_D$ → C_D discharge from V_{BIAS} to V_{BD} through R_D with a time constant $\tau_{discharge}$ ~ $R_D \times C_D$
2. Avalanche quenching → current flows to the external circuit up to a value limited by R_Q → diode current I_D decreases bellow a critical value I_{latch} ~ $(V_{BIAS} - V_{BD})/(R_Q + R_D)$ (I_{latch} limits the low values of R_Q to O(100 kΩ)
3. Diode recharge (switch open), C_D charge from V_{BD} to V_{BIAS} with a time constant $\tau_{recharge}$ ~ $R_Q \times C_D$ (since $R_Q >> R_D$, $\tau_{recharge} >> \tau_{discharge}$

SiPM equivalent circuit is more complicated

- Few more elements have to be added
  - Parasitic capacitance of quench resistor C_Q (R_Q is integrated on the same silicon substrate as the diode)
  - Parasitic capacitance of neighboring cells (SiPM is an array of GM-APDs)
  - Parasitic grid capacitance (package, wire bonding etc)

SiPM μcell eq. circuit based on Haitz model

SiPM eq. circuit connected to ext. circuit

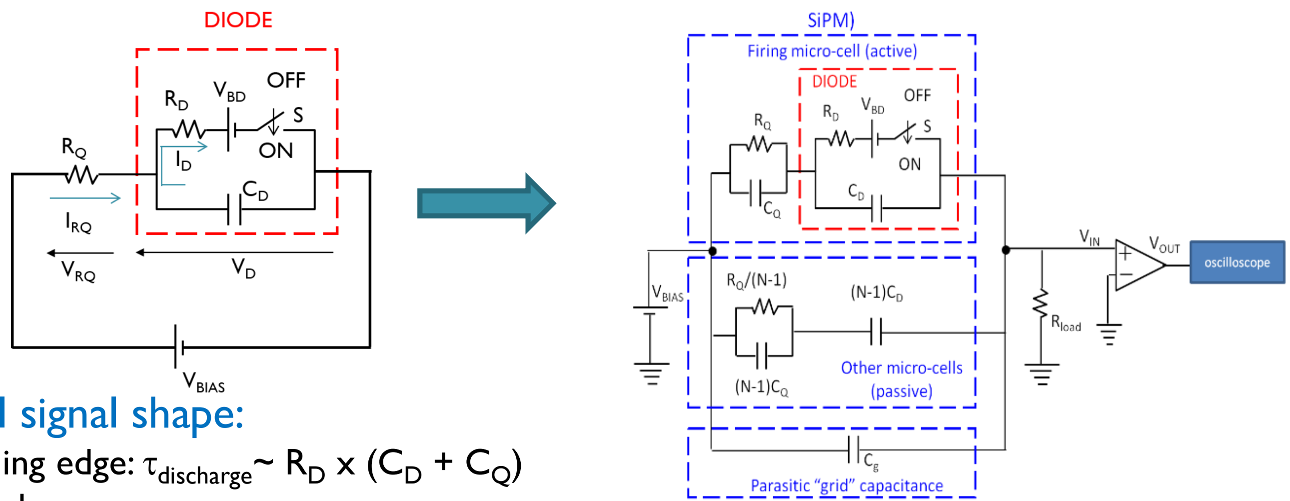

- SiPM μcell signal shape:
  - Fast leading edge: $\tau_{discharge} \sim R_D \times (C_D + C_Q)$
  - Trailing edge
    - Fast (capacitive) component: $\tau_{recharge\text{-}fast} \sim R_{LOAD} \times (C_{tot} + C_g)$
    - Slow (resistive) component: $\tau_{recharge\text{-}slow} \sim (R_Q + R_{LOAD}) \times (C_D + C_Q) \sim R_Q \times (C_D + C_Q)$

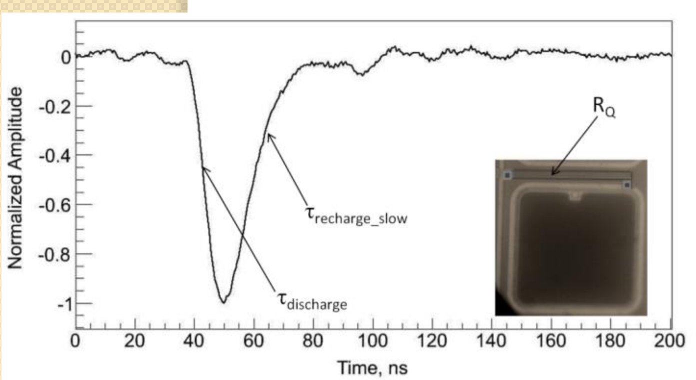

R_Q outside of diode area; no visible fast component

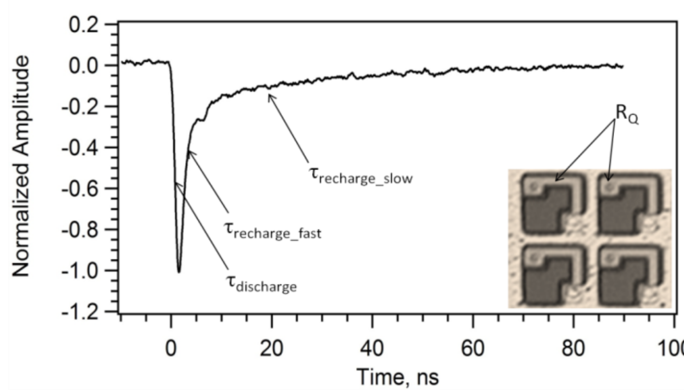

R_Q overlapping the diode area; visible fast component

$\tau_{discharge} \sim O(10\text{-}100\ ps)$

$\tau_{recharge\text{-}fast} \sim O(100\ ps)$

$\tau_{recharge\text{-}slow} \sim O(10\text{-}100\ ns)$

Signal shape and R_Q vs. temperature

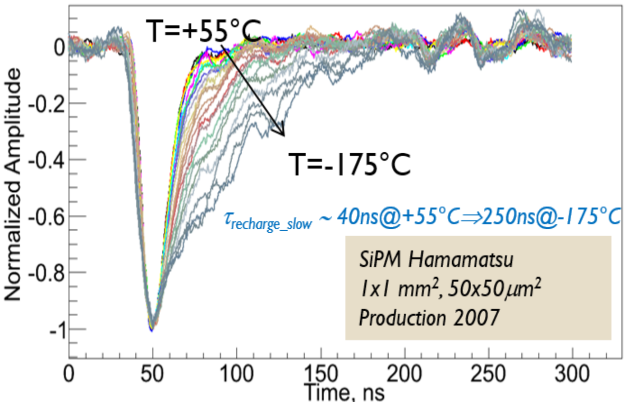

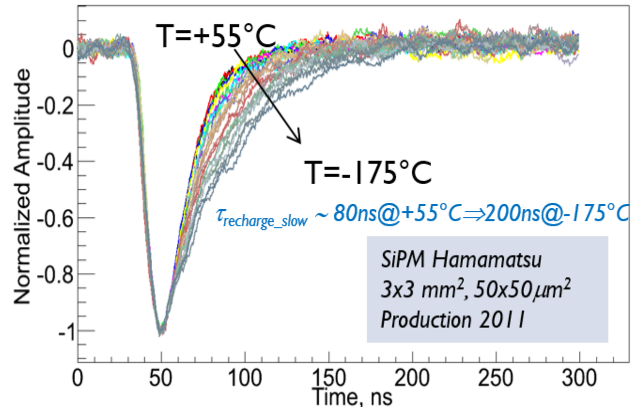

N. Dinu, A. Nagai, A. Para, NIM A 787, 2015

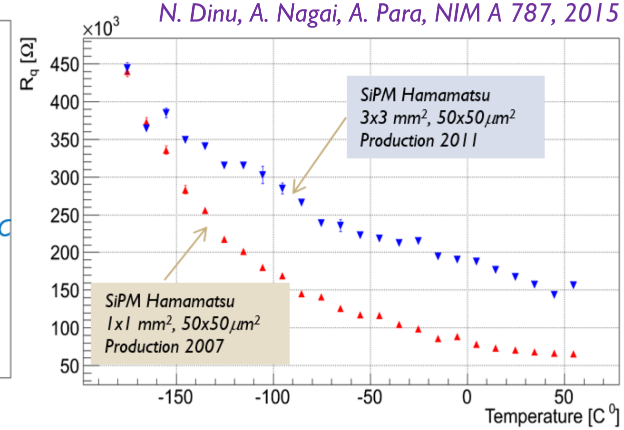

R_Q increases with decreasing temperature (negative T coefficient)

⇒ Slow recharge time component ($\tau_{recharge\text{-}slow} = C_{\mu cell} \cdot R_Q$) increases with decreasing T

HPK MPPC: 25μm, 50μm, 100μm

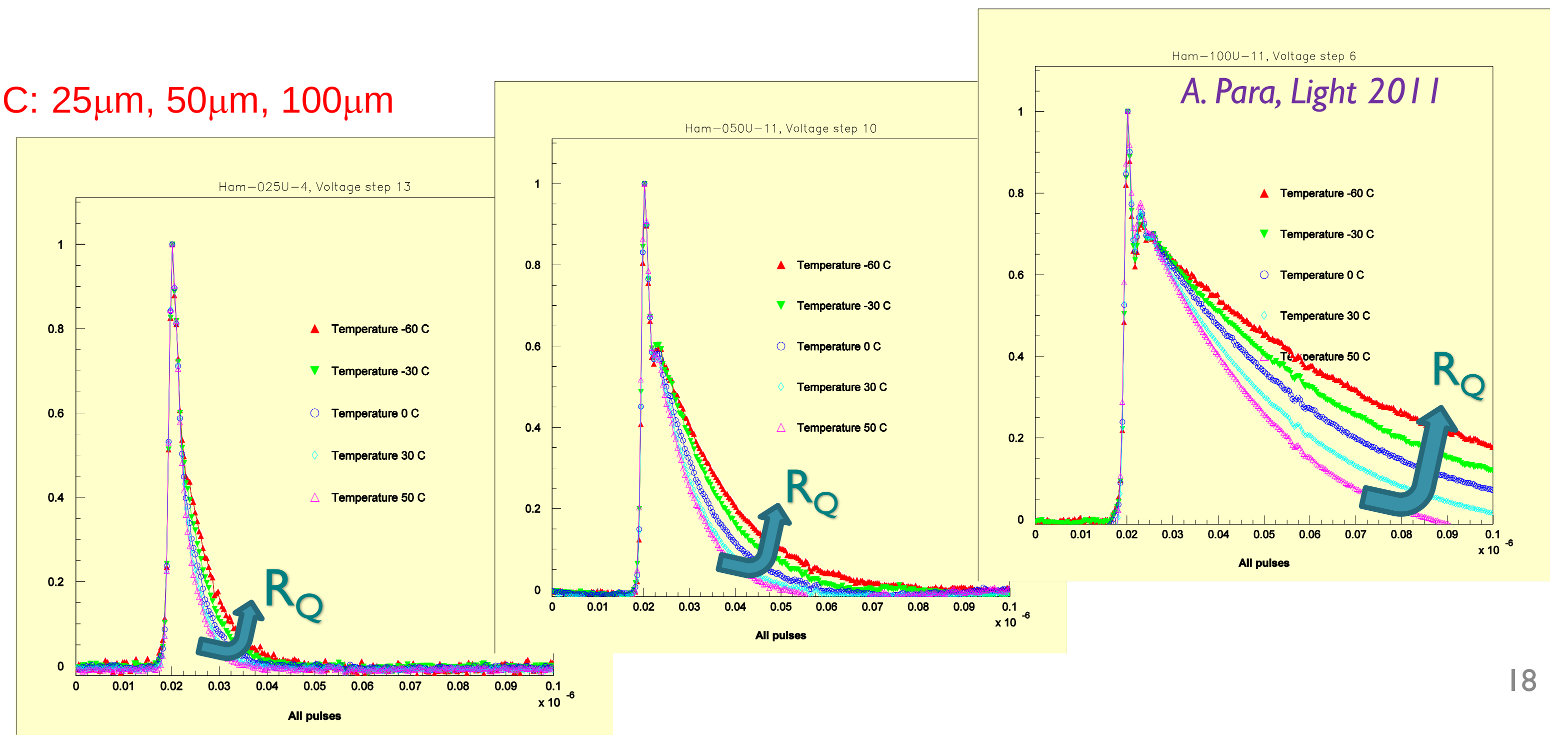

Examples of signal shape improvements

HPK

Thin metal film quenching resistance (MQR)

- Lower T dependence than poly-Si quench resistor

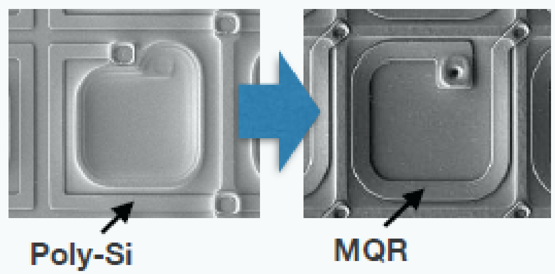

K. Sato et al., IEEE TNS 2013

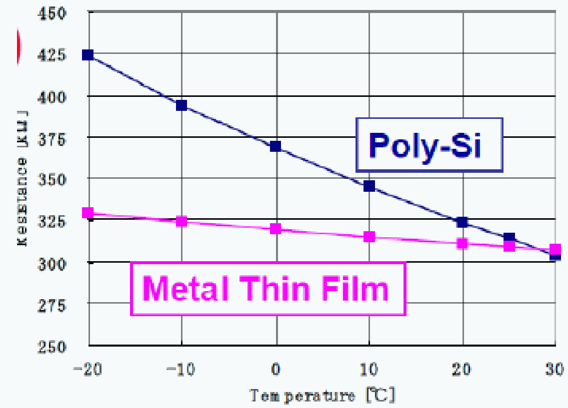

SensL

Each junction has a connection to a third electrode with a low capacitive coupling

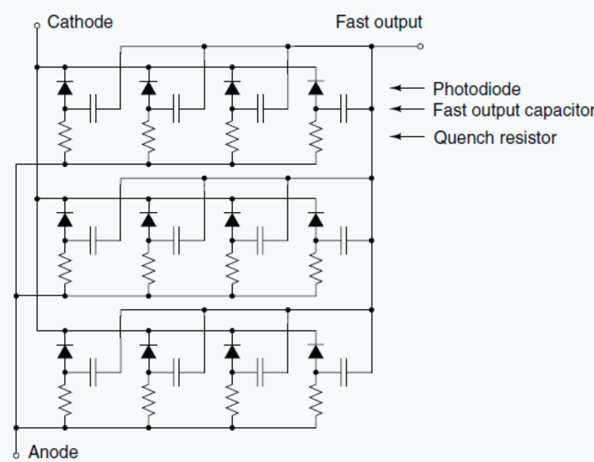

B-series SiPM circuit schematic

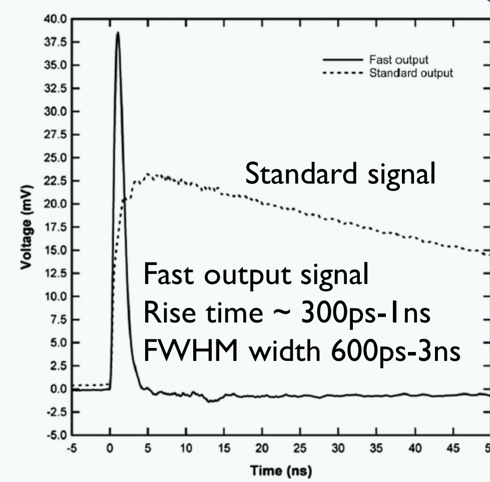

C. Jackson, Opt. Eng. 53(8), 2014

SiPM timing resolution

- Time jitter between the true arrival time of the photon at the sensor and the instant when the output current pulse is recorded
- Two components :
  - fast component of gaussian shape with σ *O*(100ps)
    - due to photons absorbed in the depletion region
    - its width depends on the statistical fluctuations of the avalanche build-up time (e.g. photon impact position → cell size)
  - slow component: minor non gaussian tail with time scale of *O*(ns)
    - due to minority carriers, photo-generated in the neutral regions beneath the depletion layer that reach the junction by diffusion (wavelength dependent)

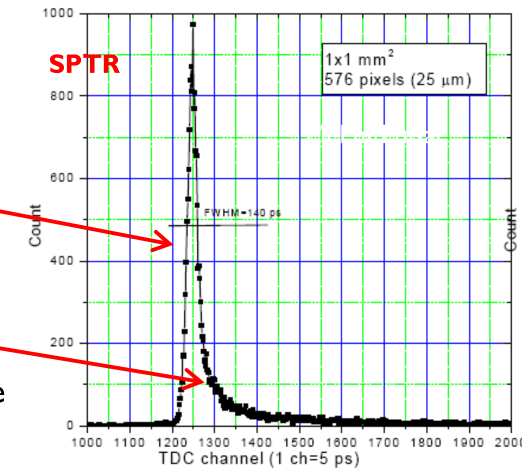

Courtesy of G. Collazuol (not published)

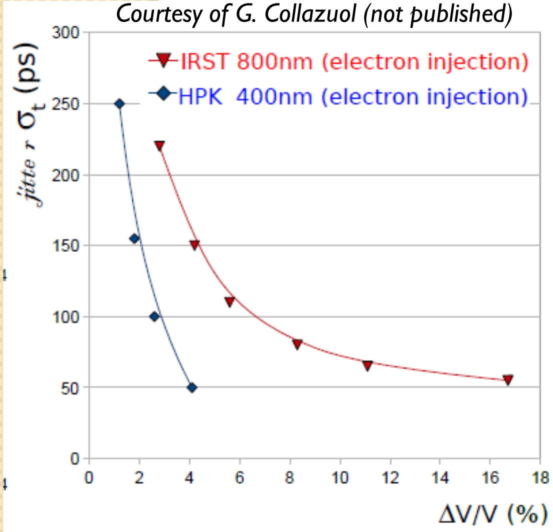

G. Collazuol et al., NIM A, 581, 2007

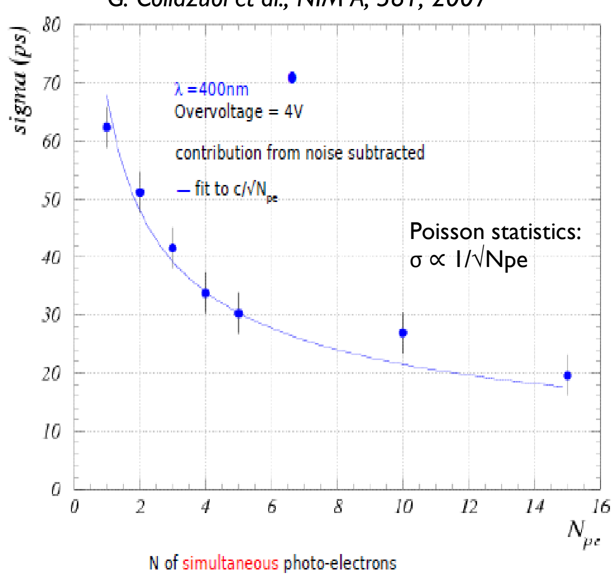

Fast plastic scintillator (BC422 60×30×5mm³) readout by 6 SiPMs

P. W. Cataneo, WO, et al. IEEE-TNS 61(2014)2657

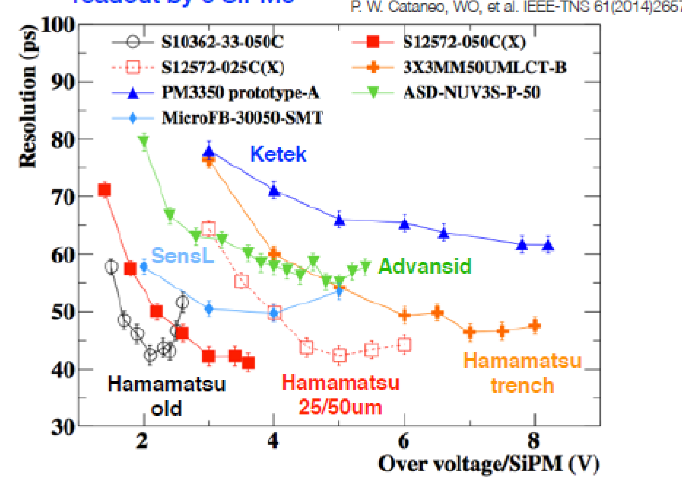

- Better resolution at higher ΔV (gain, PDE)
- Saturated due to dark noise or afterpulsing

SiPM linearity/ saturation

- Good linearity as long as $N_{photons} < N_{\mu cells}$
- Main sources of non-linearity:
  - finite number of cells - main contribution when $N_{photons} \sim O(N_{cells})$
  - recovery time (large number of photons arriving in a time interval shorter than recovery time)
  - afterpulses, cross-talk
  - drop of ΔV during the light pulse due to relevant signal current on external series resistance

Response of various SiPM's with different total number of μcells measured with 40ps laser pulses

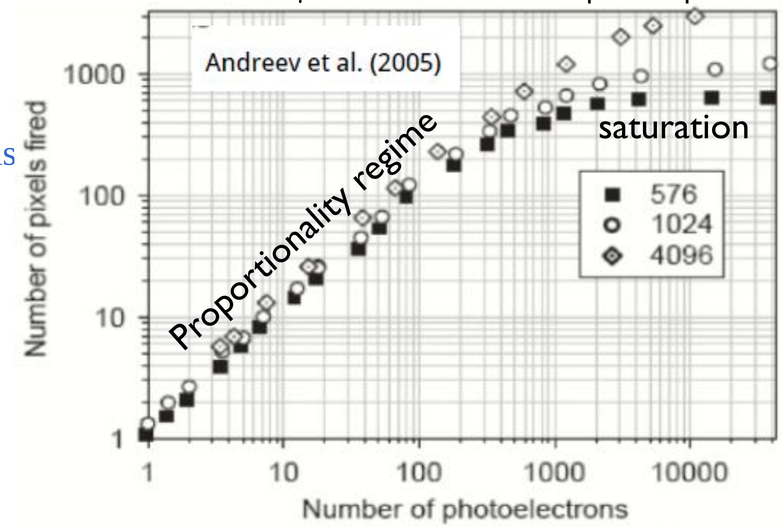

20% deviation from linearity if 50% μcells fired

$$N_{firedcells} = N_{total} \cdot \left(1 - e^{-\frac{N_{photon} \cdot PDE}{N_{total}}}\right)$$

- Need to choose the devices with cell density that meets the application requirements
- Rule of thumb for device choose:
  - Number of photons per μcell < 1

Symplified model: Stoykov, & al., JINST June, 2007
Detailed model to estimate non-linearity corrections: T. van Dam & al., IEEE TNS 57 (2010) 2254

Improvements to SiPM linearity – small μcells size

- 10 μm cell pitch from Hamamatsu SiPM
  - Fill factor improved by metal quench resistor (MQR)
  - Thin MQR (transparent to light) over active area

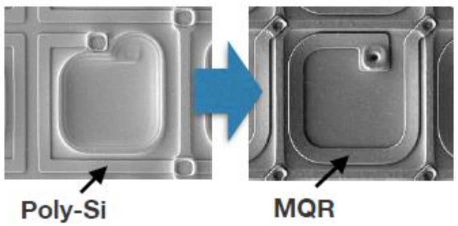

K. Sato et al., IEEE TNS 2013

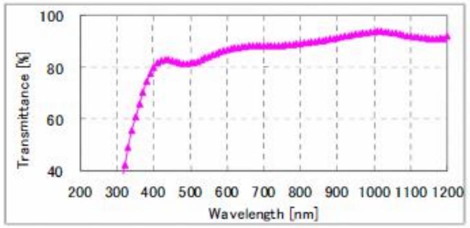

T.Nagano et al., IEEE TNS 2011

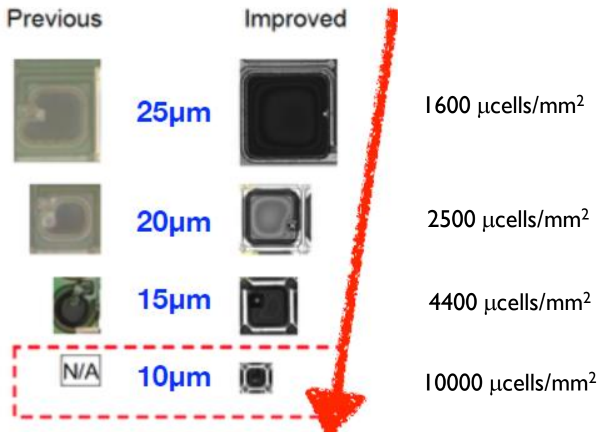

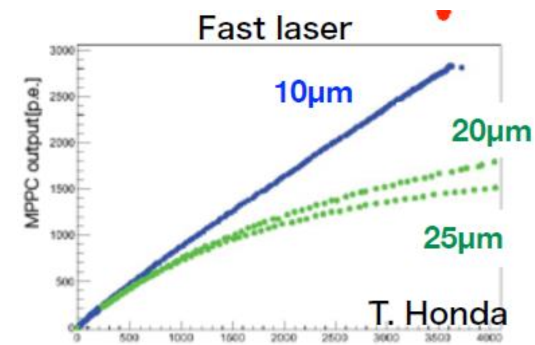

- 15 μm cell pitch from KETEK and AdvanSiD

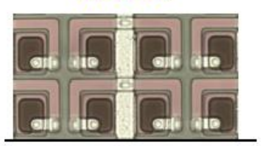

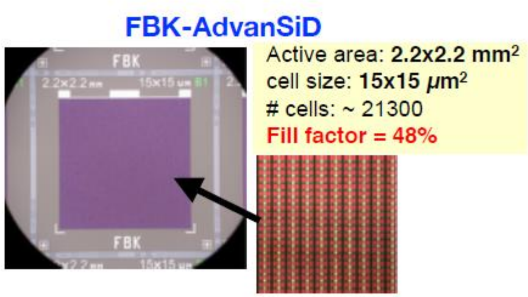

- Micro-cells from Zecotek, Amplification tech
  - Up to 40000 cells/mm²

Zecotek
Sadygov et al arXiv 1001.3050
Sadygov RU Patents № 1996/2102820 and № 2006/2316848

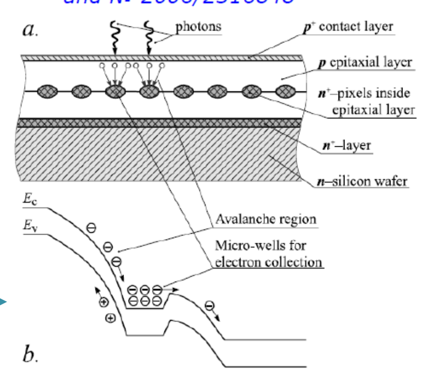

Nicoleta Dinu - Jaeger, LAL-ARTEMIS, CNRS, Brussels Seminar, 04.03.2016

GAIN

Defined as the charge developed in one μcell by a primary charge carrier:

$$G = \frac{Q}{q_e} = \frac{(C_D + C_Q)\Delta V}{q_e} = \frac{(C_D + C_Q)(V_{BIAS} - V_{BD})}{q_e} = \frac{C_{\mu cell}(V_{BIAS} - V_{BD})}{q_e}$$

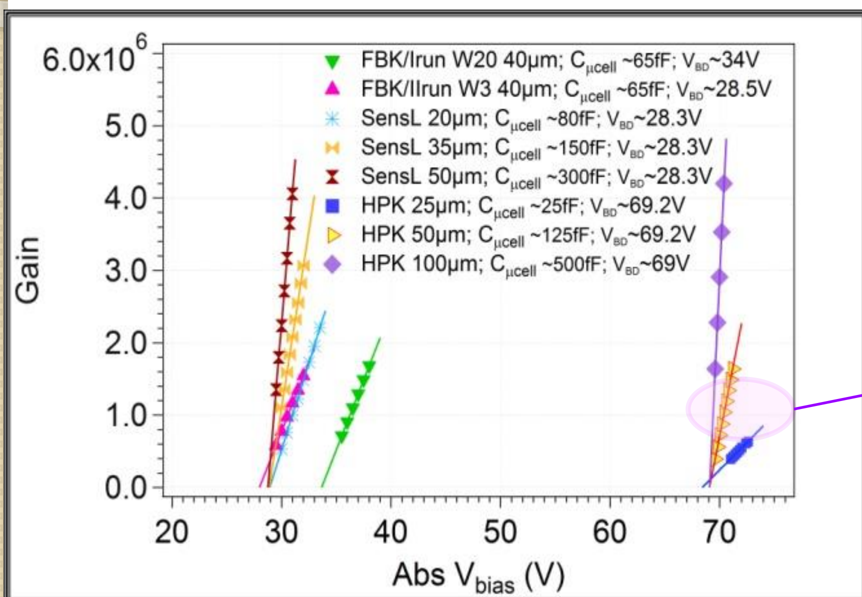

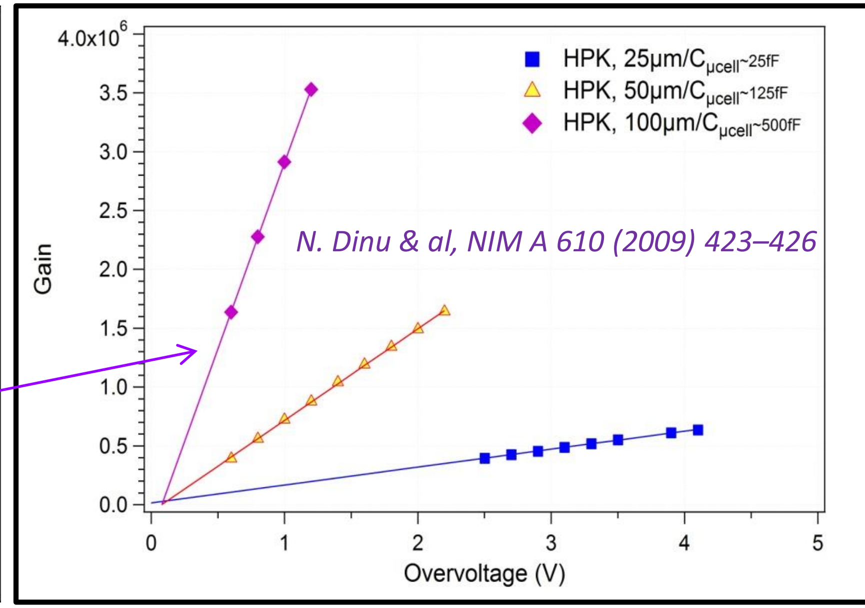

- G increases linearly with V_{BIAS} at a given V_{BD}
  - G: $5\text{x}10^5 - 5\text{x}10^6 \Rightarrow$ simple read-out electronics required
- The slope of the linear fit of G v.s. $\Delta V \Rightarrow$ μcell diode capacitance
  - $C_{\mu cell}$: tens to hundreds of fF
- G and C_D increase with the μcell geometrical dimensions
  - $C_D \sim \varepsilon_0 \varepsilon_r S/d$; S - μcell junction surface; d - μcell depletion thickness

Gain vs. bias voltage vs. temperature

N. Dinu, A. Nagai, A. Para, NIM A, 787 (2015)

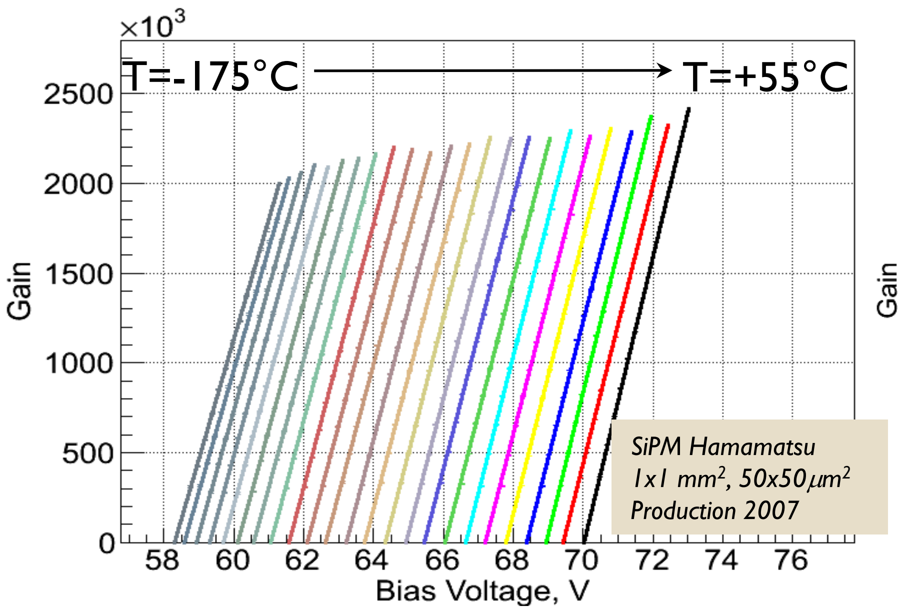

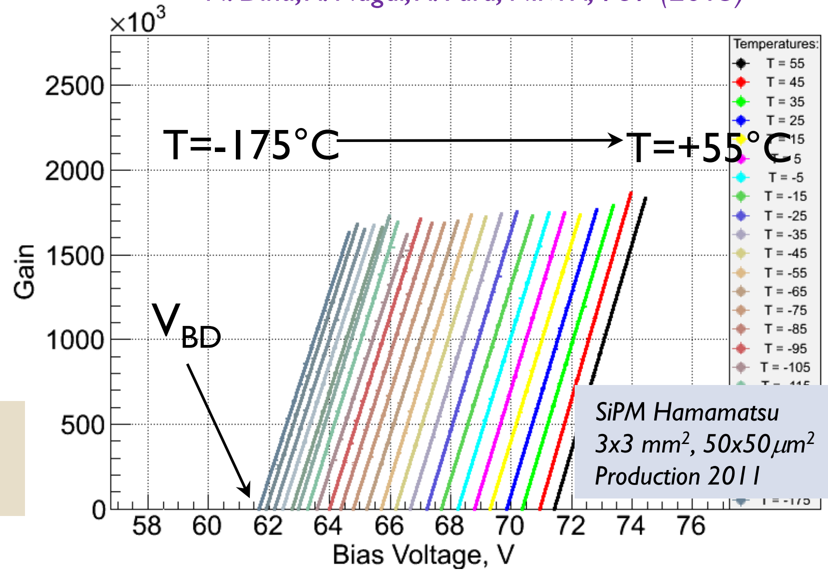

Gain variation with T is determined by V_{BD} variation with T

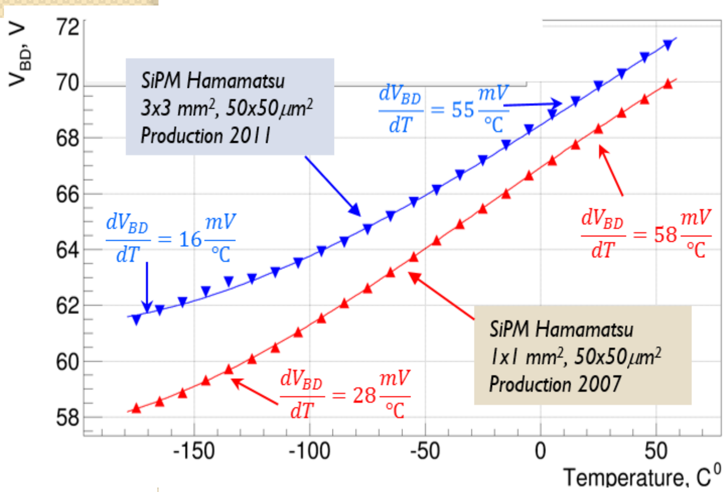

Better V_{BD} stability at low T

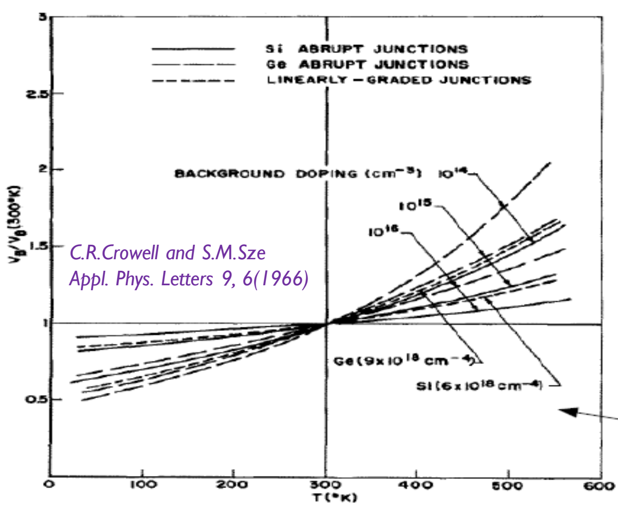

T dependence of V_{BD} can be tuned by varying the doping concentration & thickness of epi layer

- **Early devices (2007-2011)**
  - T in the range from -20°C to +20°C
    - dV_{BD}/dT (HPK) ~ 55-60 mV/°C
    - dG/dT ~ 2.7%/°C for ΔV=2V

Present generation (2015):

- dV_{BD}/dT (HPK) ~ 55 mV/°C
- dV_{BD}/dT (KETEK) ~ 22 mV/°C
- dV_{BD}/dT (FBK) ~ 25 mV/°C
- dV_{BD}/dT (SensL) ~ 21.5 mV/°C

- Devices work at higher ΔV
- dG/dT ≤ 1%/°C for ΔV=5V

Gain vs. overvoltage vs temperature

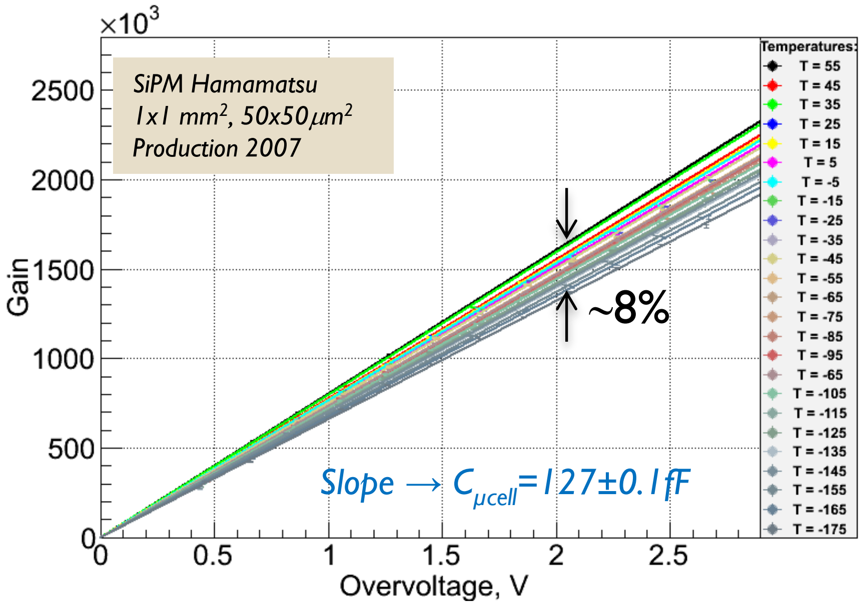

N. Dinu, A. Nagai, A. Para, NIM A, 787 (2015)

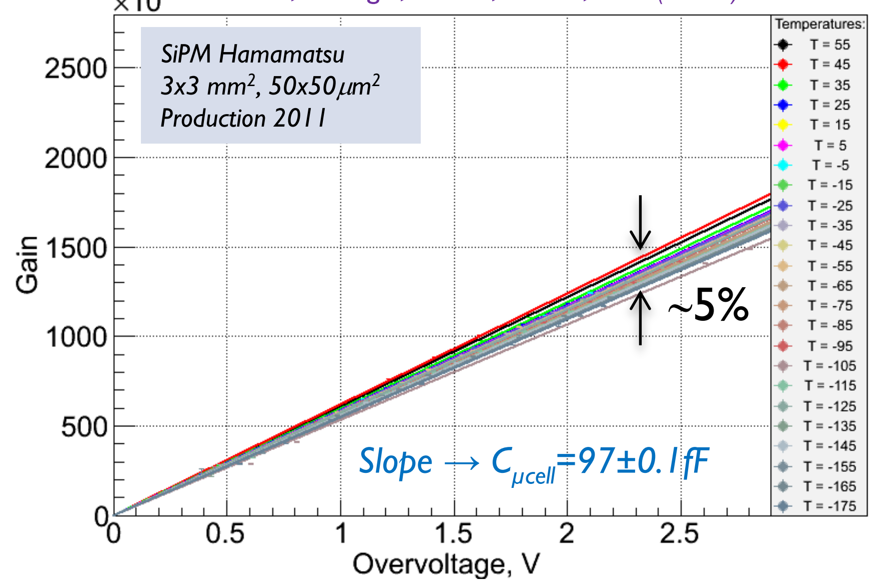

Capacitance vs. temperature

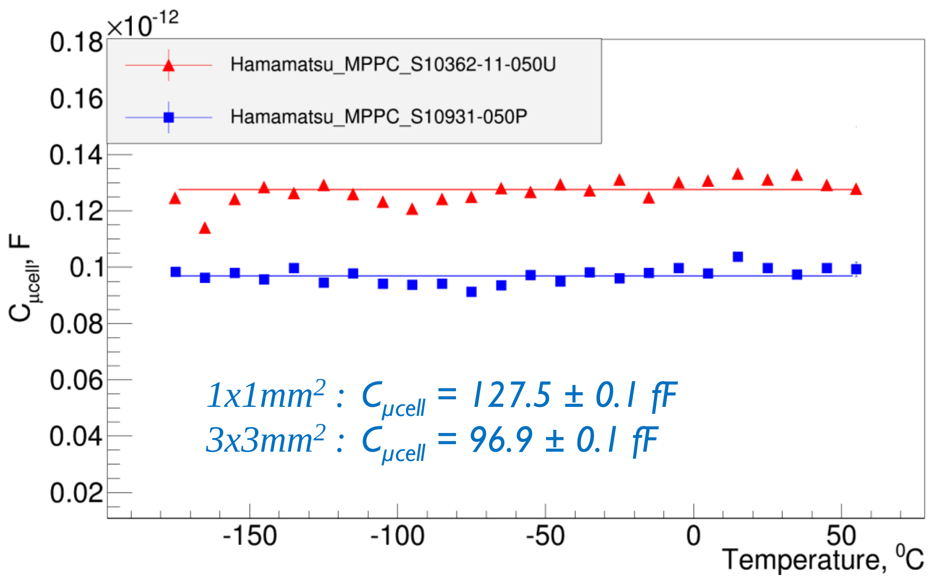

- Gain independent of T at fixed ΔV
- $C_{\mu cell}$ is independent of T
  - the difference of two $C_{\mu cells}$ values is related to ~20% μcell area difference between two devices

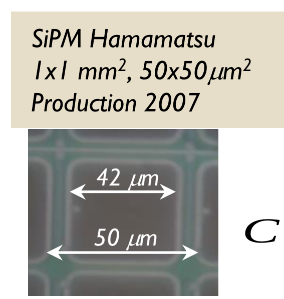

$$C = \varepsilon_{Si}\varepsilon_0 \frac{A}{d}$$

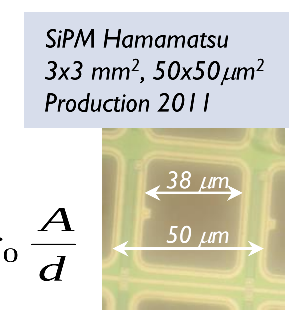

Dark count rate (I)

- The number of pulses/s registered by the SiPM in the absence of the light
- It limits the SiPM performances (e.g. single photon detection, linearity, timing resolution)
- **Three main contributions:**

Primary pulses (uncorrelated) triggered by:

- Thermal (SRH)
- Trap-assisted & band-to-band tunneling
  - carrier generation in the depleted region

  ⇔ ***looks the same as a photon pulse***

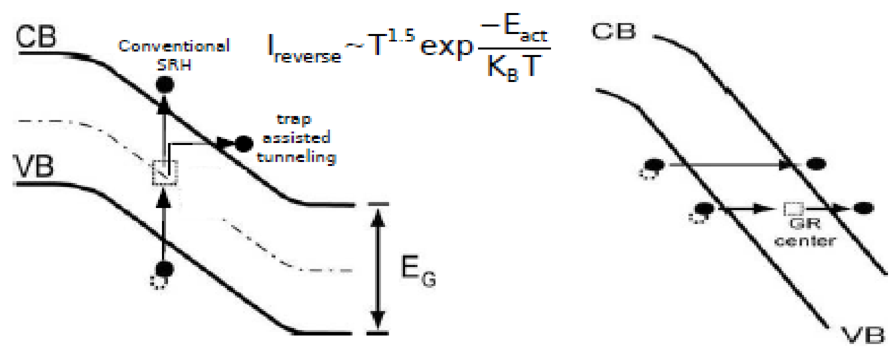

Secondary pulses (correlated):

- After-pulses
  - carriers trapped by deep level defects during the avalanche discharging and then released, they trigger a new avalanche after the breakdown

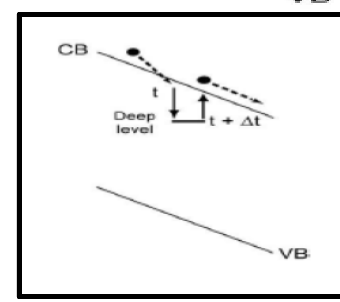

- Optical cross-talk
  - photons emitted during avalanches (thermo-luminescence)
  - these photons can trigger an avalanche in an adjacent μcell
  - Various mechanisms
    - direct cross-talk (instantaneous)
    - << 1ns
  - Indirect cross-talk (delayed)
    - 10-100 ns

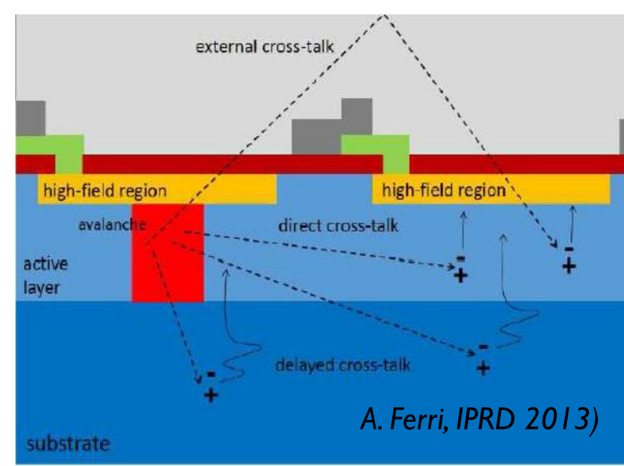

A. Ferri, IPRD 2013)

Dark count rate (2)

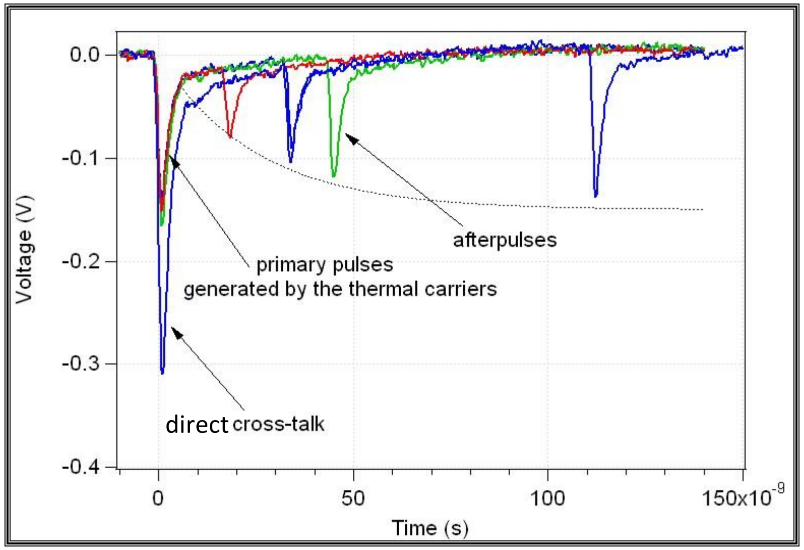

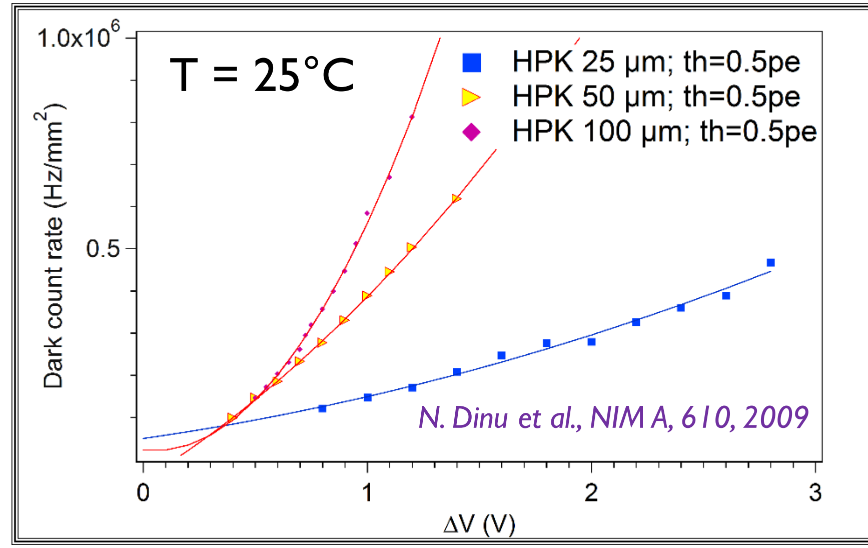

DCR

- linear dependence due to triggering probability $\propto \Delta V$
- non-linear at high ΔV due to cross-talk and after-pulses $\propto \Delta V^2$
- scales with the active area (it should be mentioned /mm^2)
- Critical issues:
  - Quality of epitaxial layer
  - Quality of Si substrate
  - Gettering techniques
  - Electrical field → tunneling

- Most recent devices
  - DCR < 50 kHz/mm^2

Trend is higher PDE and lower DCR

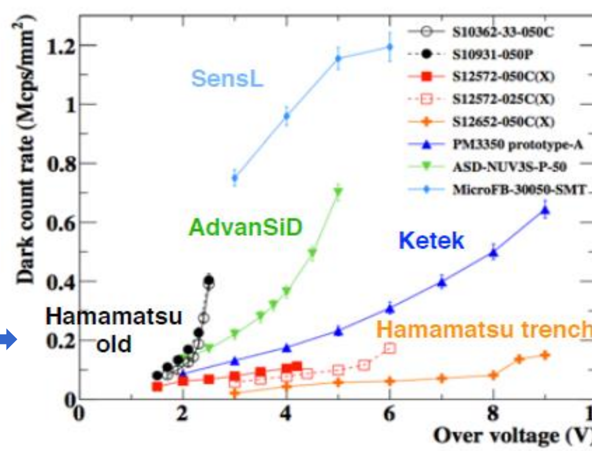

P. W. Cataneo, WO, et al. IEEE-TNS 61(2014)2657

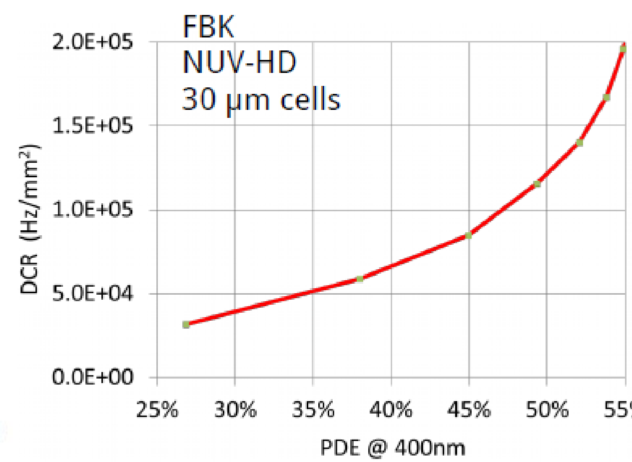

NOTE: DCR depends on overvoltage, as well as PDE
→plotting DCR vs PDE yields fairer comparison

Dark count rate vs. temperature

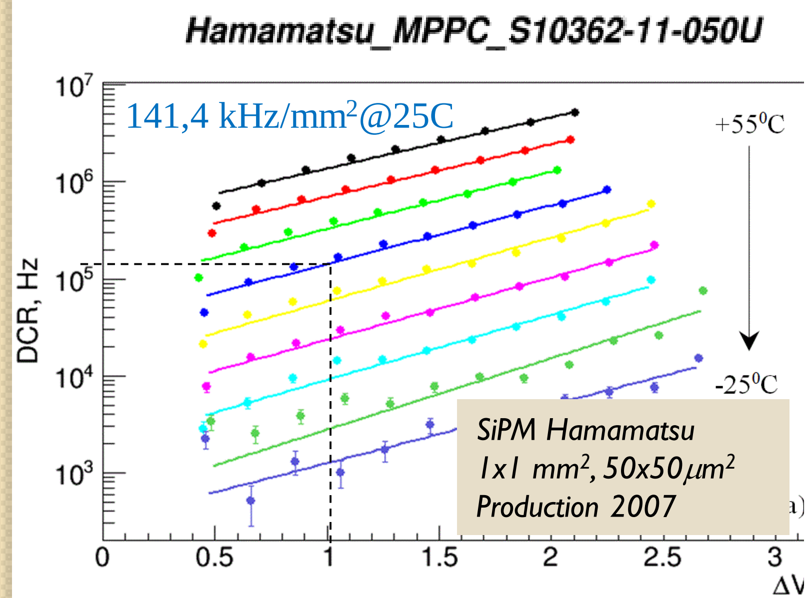

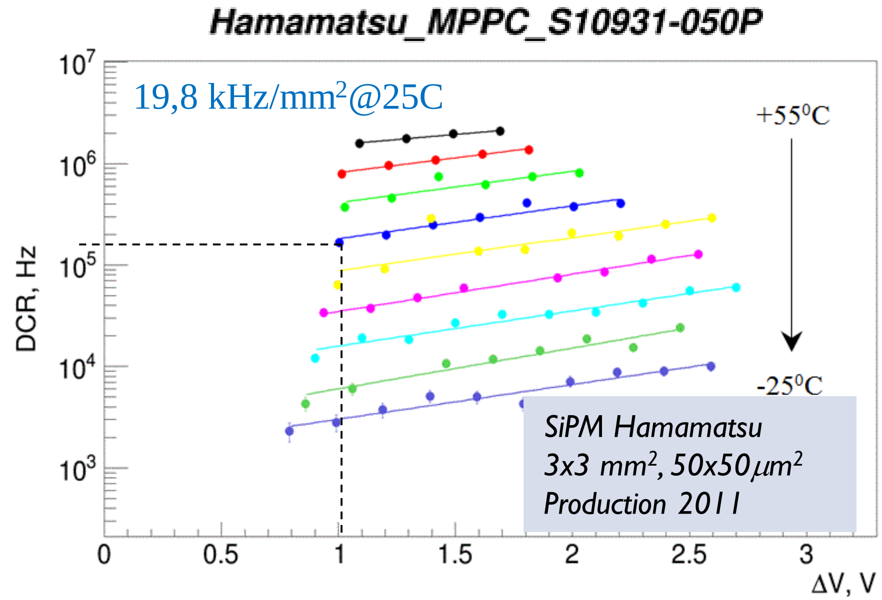

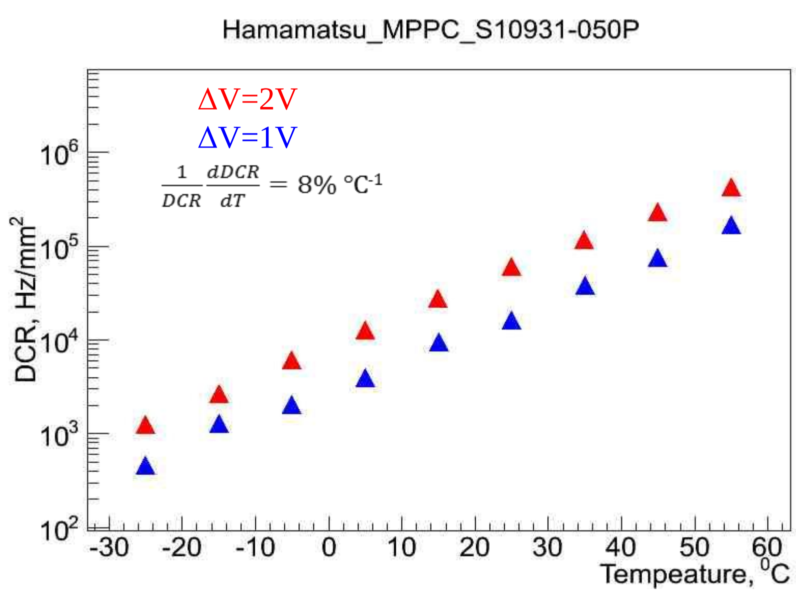

A low-electric field NUV-HD version has been developed to reduce the tunnelling component of the DCR.

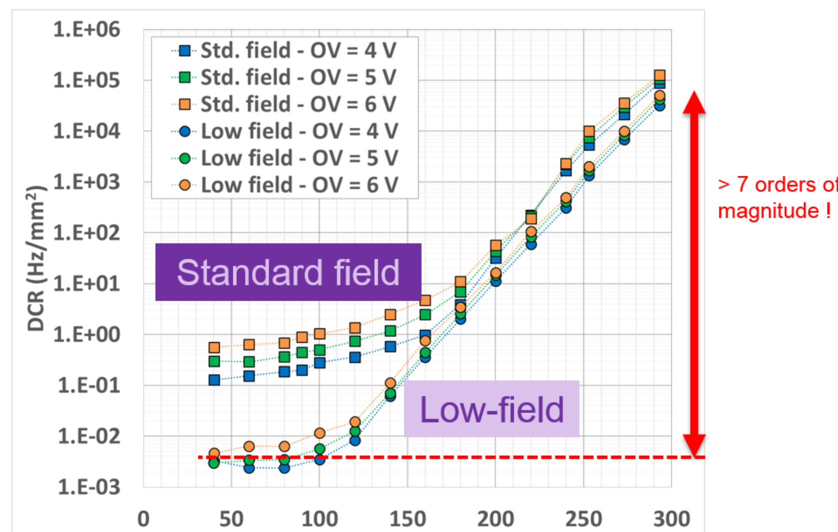

From Zappala & al., VCI, 2016

Summary of various detectors characteristics

	PIN	APD	GM-APD	SiPM
Gain	1	10^2 - 10^4	$\geq 10^6$	$\geq 10^6$
Single photon detection / light intensity	no yes	no yes	yes no	yes yes
Op. voltage	0-5V	0.1-1kV	20-500V	<70V
Temp. sensitivity	low	high	low	low
Mech. Robustness	high	medium	high	high
Ambient light	o.k.	o.k.	o.k.	o.k.
Spectral range	tunable	tunable	tunable	tunable (NUV-IR)
Readout electronics	simple/complex	complex	simple	simple
Form factor	small	small	small	compact
Cost	low	high	low	low
Large area	no	no	no	Scalable
Magnetic field sensitivity	no	no	no	no
Noise	low	medium	low	Medium (improvements)
Response time	fast	slow	fast	fast
Detection efficiency	QE>90%	QE~80-90%	QE x P_{geiger} 80-90%	QE x P_{Geiger} x ε_{geom} Peak: 40-75%

SiPM is almost a perfect detector for visible light

PART B:

SiPM applications

Techniques of nuclear imaging

- ## Principle

Marking

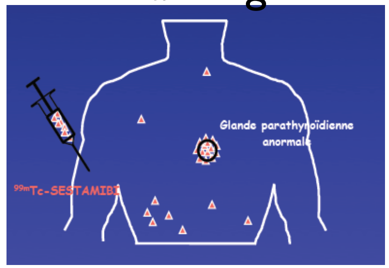

Detection

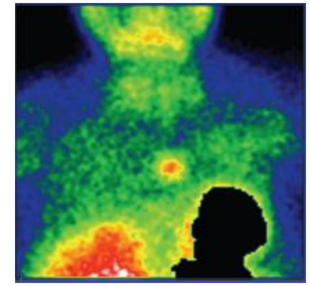

Pharmaceutical product:

- organic molecules + radioactive isotope
- Radioactive isotopes
  - ^{99m}Tc, ^{123}I, ^{201}Tl, ^{18}F, ^{11}C
  - Emitters γ, β^+ or β^-

Techniques of nuclear imaging

- γ camera, topographies

- ## Techniques

Cancer diagnostic (homographs)

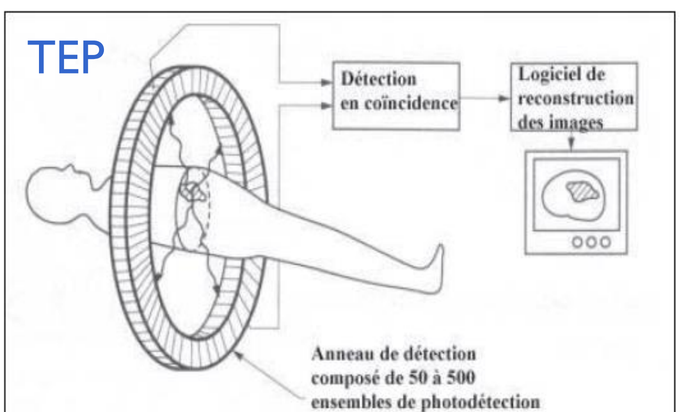

Cancer therapy (Per-operative detection systems)

- Gamma probes
  - ergonomic shape (pencil)
  - 1-2 cm diameter, 10-20 cm length
  - sound signal proportional to counting rate
- Gamma imaging cameras
  - cover larger area: 10-100 cm^2
  - give the spatial distribution of the radio-tracer
  - improve signal to noise ratio

POCI/TRECAM, France

Sentinella, Spain

MAGICS camera

N. Dinu et al., NDIP 2014
NIM A, 787, (2015), 367-372

- High resolution hand-held radiation detector for therapeutic purposes

Radio-guided surgery

MAGICS imaging camera

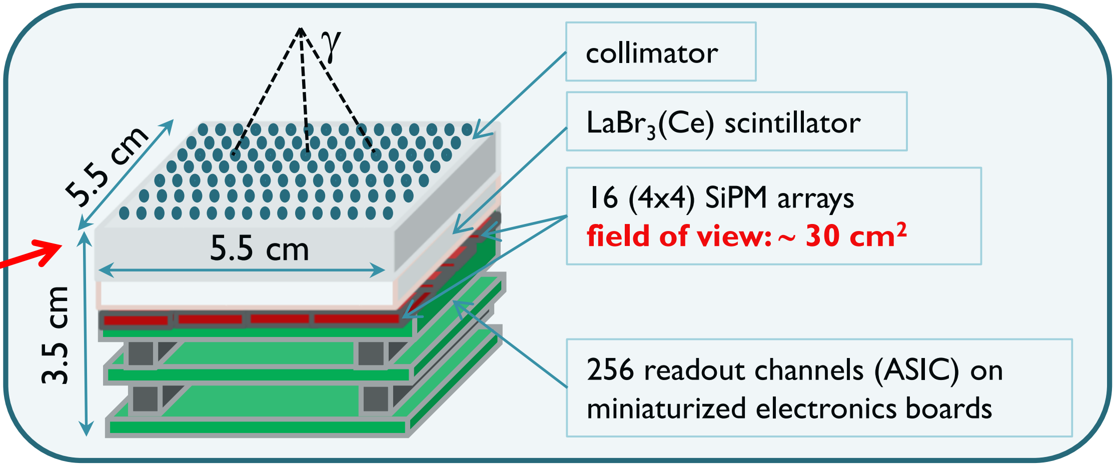

Collaboration IMNC, LAL, Hôpital Lariboisière

Detection system requirements in surgical conditions
- reduced size and weight
- versatility of readout electronics
- adapted for sterile environment

S11828-3344M Hamamatsu HPK
- 4x4 monolithic SiPM array (earliest arrays on the market)
- mounted on a SMD package
- Each SiPM = one readout channel:
  - 3x3 mm^2, 3600 μcells, each μcell - 50x50 μm^2

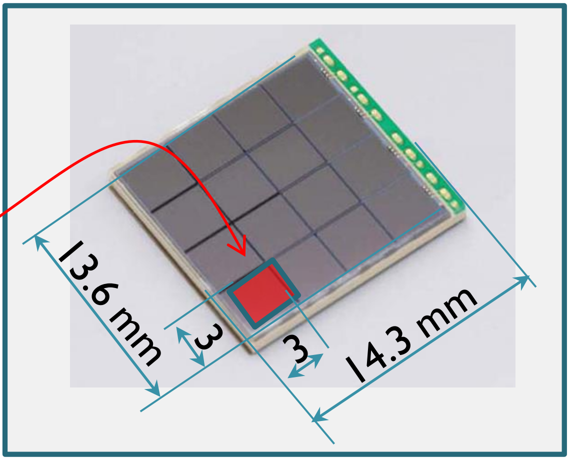

i-v measurements of monolithic SiPM arrays

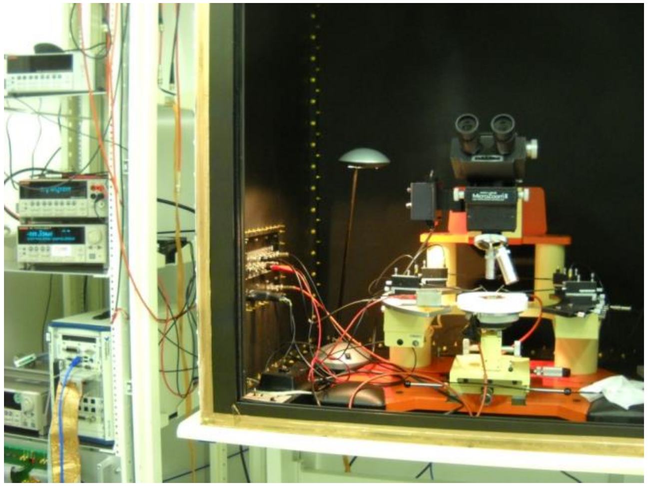

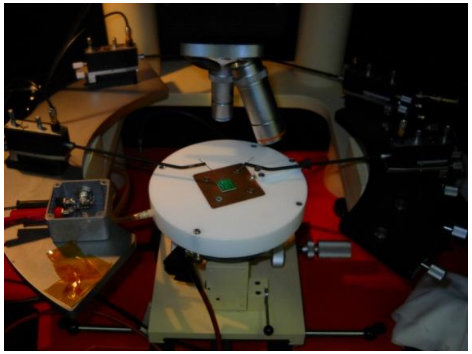

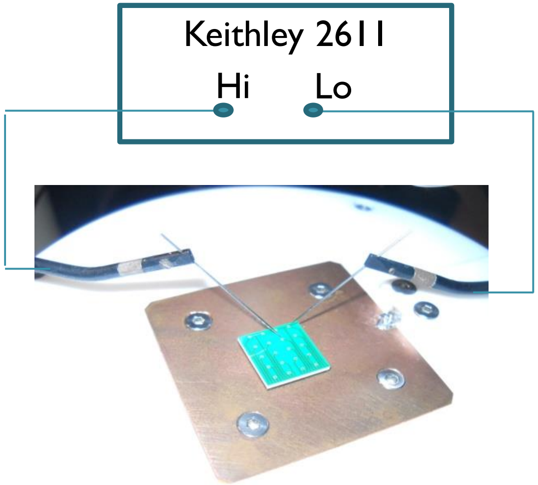

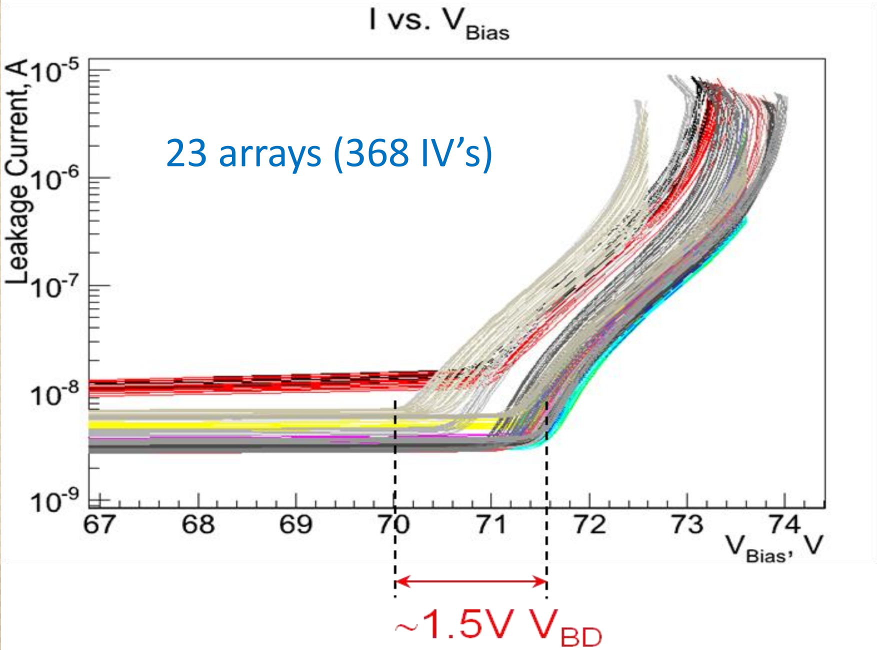

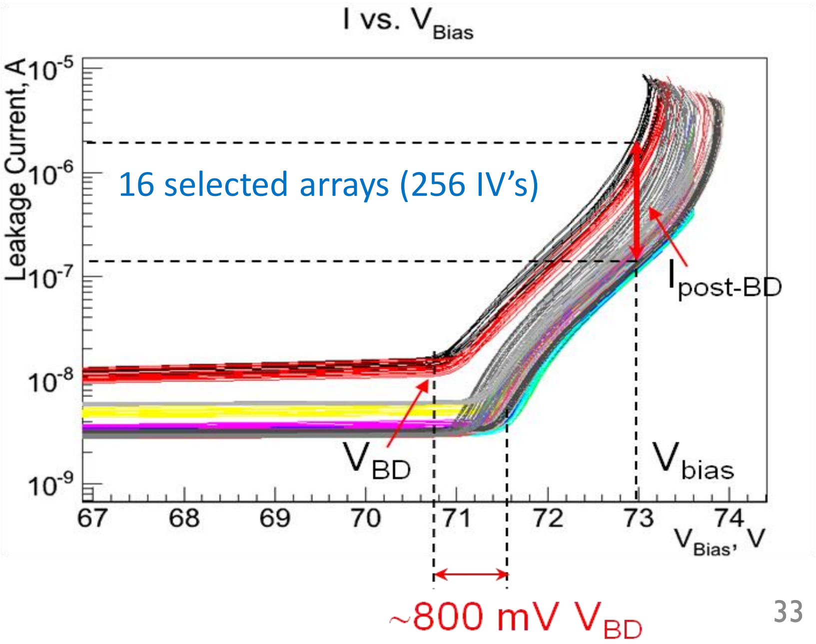

SiPM characteristics uniformity

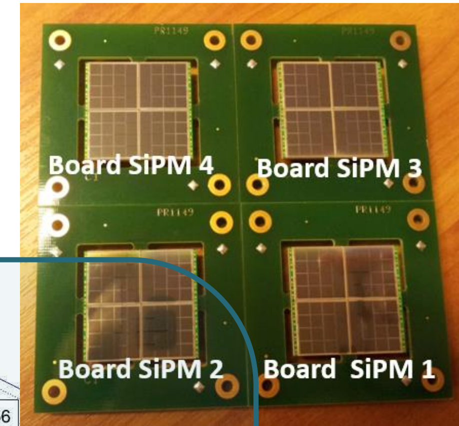

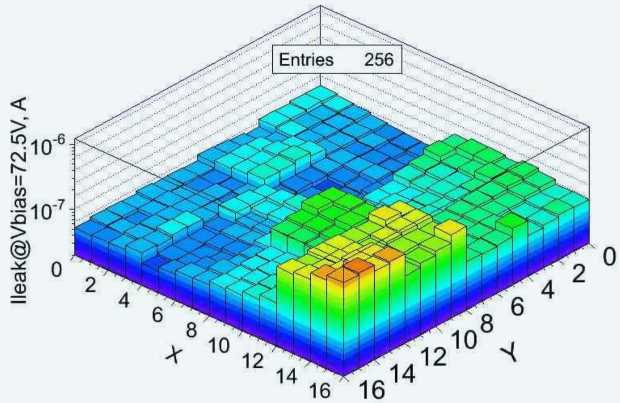

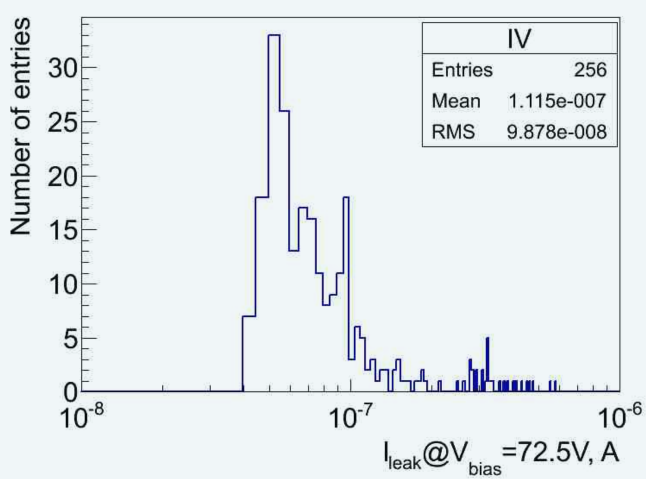

common V_{BIAS}=72.5V for all devices

σ_{Ileak} = 88% over 256 channels

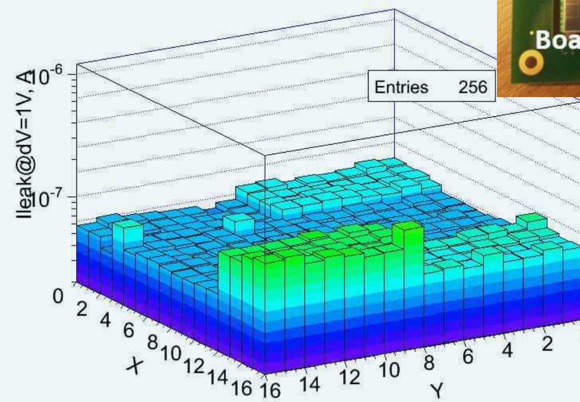

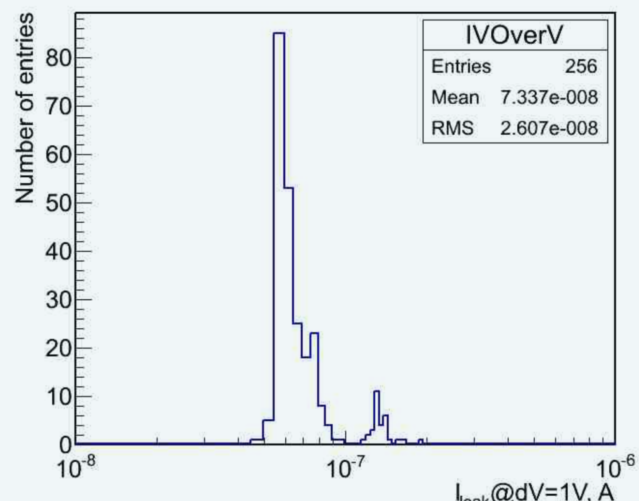

common ΔV=1V for all devices

σ_{Ileak} = 35% over 256 channels

removing the two noisy SiPM's: σ_{Ileak} = 13%

Elementary module of MAGICS camera

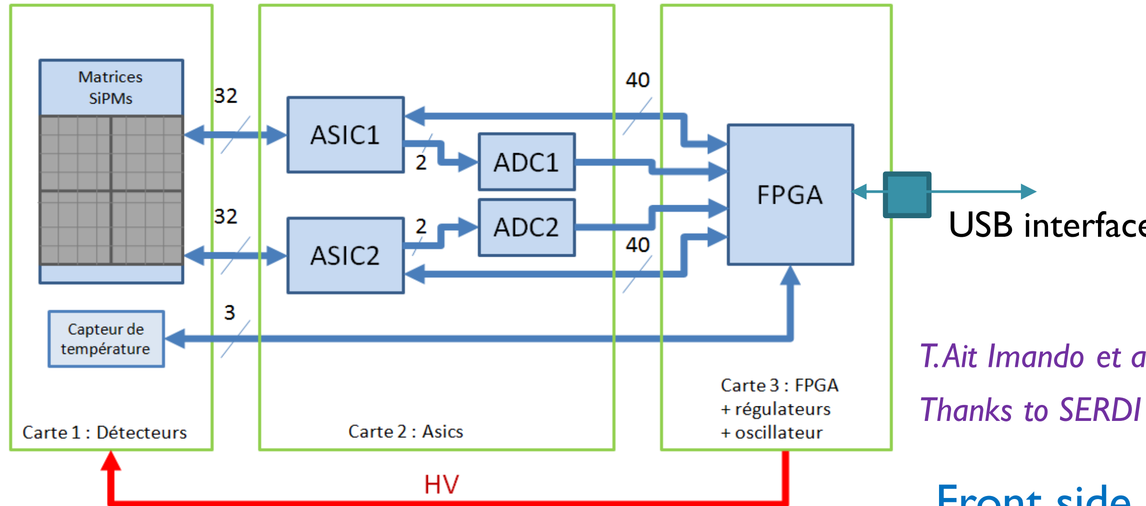

T.Ait Imando et al., PoS 2012

Thanks to SERDI (LAL) for technical help

Elementary module

Field of view: ~ 8 cm^2

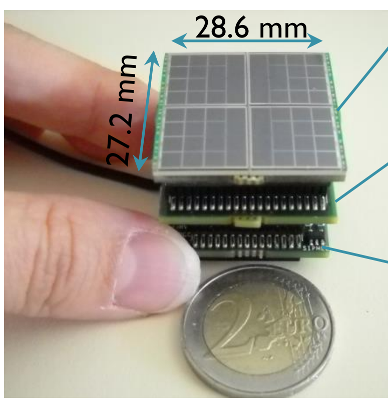

Board 1:
4 (2x2) SiPM arrays
64 channels

Board 2:
2 EASIROC chips
64 readout channels
2 ADC 12 bits

Board 3:
ALTERA ciclone III FPGA
FTDI FT2232H (USB, 2.0 Hi-speed, 440MBit/s)
DC/DC converter for SiPM bias

Front side | Back side

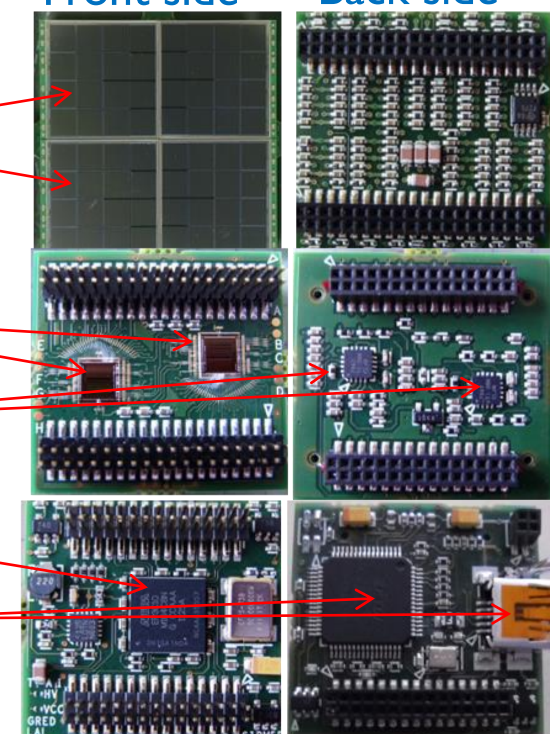

Characteristics of read-out electronics

- **EASIROC chip**
  - 32-channels fully analog front-end readout
  - 8-bit DAC (0-2.5 V) for individual SiPM gain adjustment
  - energy measurement from 160 fC to 320 pC
    - 1 to 2000 pe @ SiPM gain of 10^6
    - variable gain pre-amplifier tuned to 4 bits
    - variable shaping time from 25 to 175 ns
    - 2 multiplexed analog outputs (high gain, low gain)
    - 1 pe signal/noise ratio ≈ 9
  - Low power consumption
    - 4.84 mW/channel, 155 mW/chip

Channels uniformity for HG output
σ < 1%

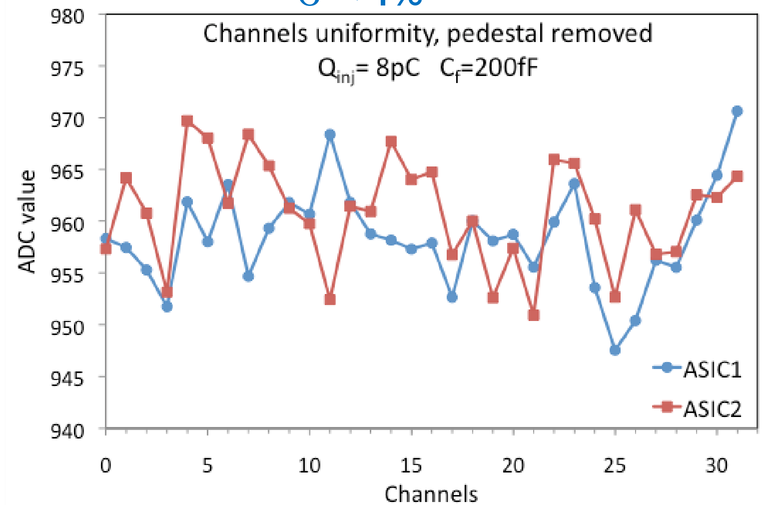

Channels linearity for HG output
σ < 1% from 160 fC to 100 pC

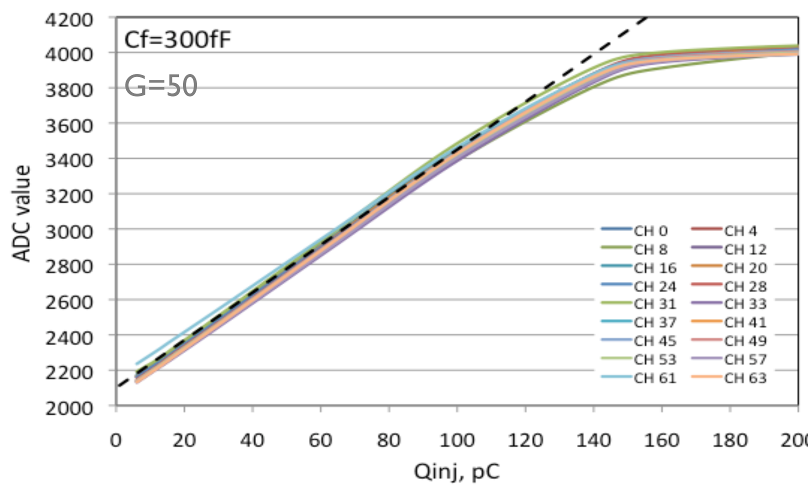

SiPM gain correction vs temperature using input DAC

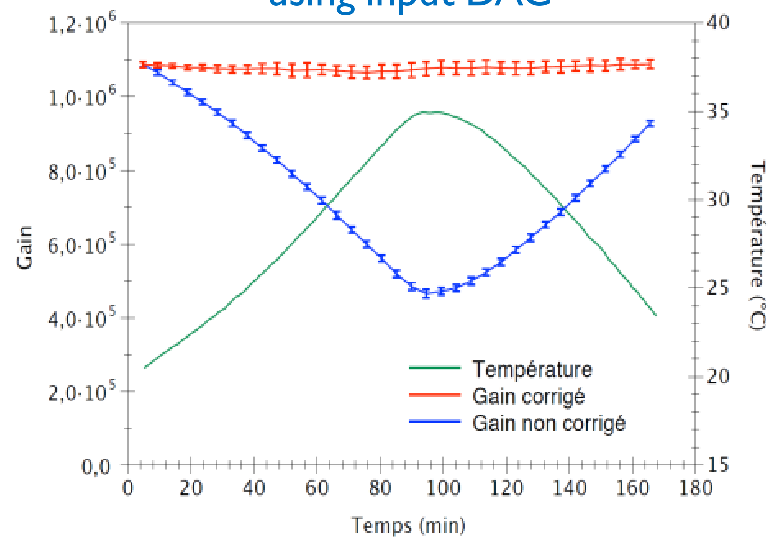

MAGICS camera

4 elementary modules
256 SiPM's = 256 readout channels

Architecture

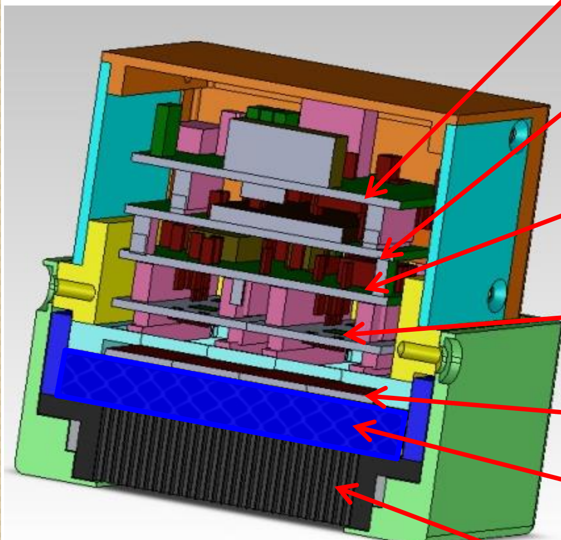

Mechanics
- *alignment and assembling*

Software
- *boards driving, data acquisition and treatment*

4 elementary modules

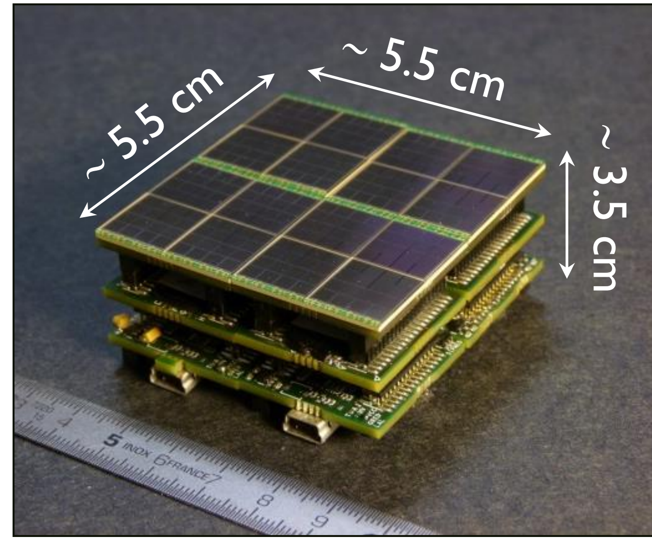

MAGICS camera final view

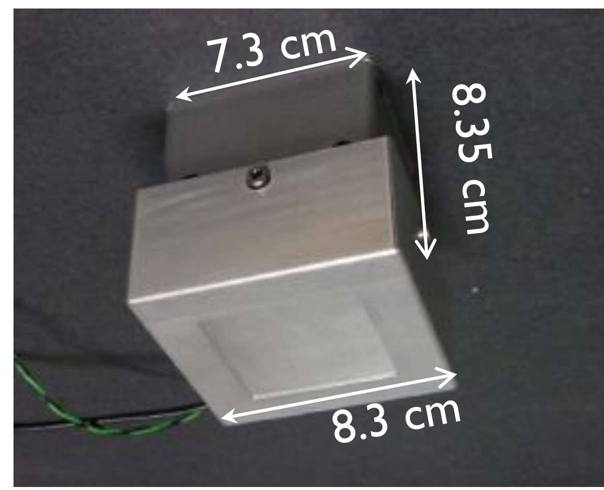

Dimensions: 8.3 x 8.3 x 8.35 cm^3
Weight: 1.2 kg
Field of view : 5.1x5.1 cm^2

Characteristics of MAGICS camera

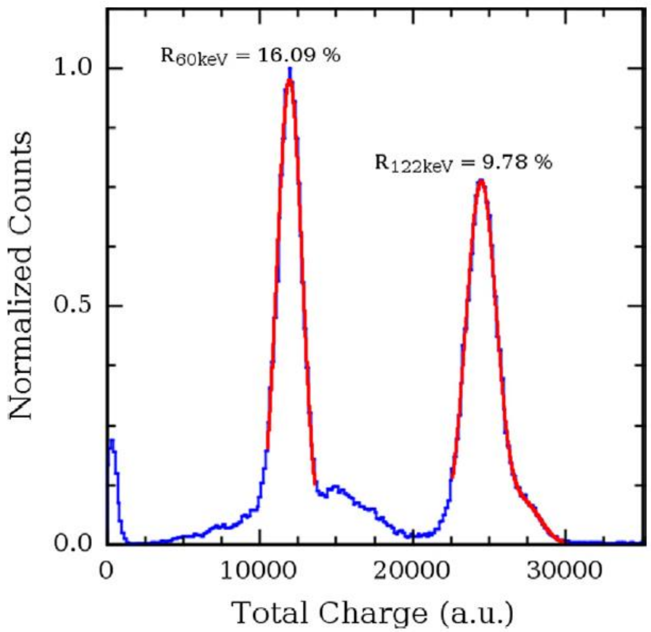

Energy resolution:

- 9.8% @ 122 keV

Experimental conditions:

- $LaBr_3(Ce)$ – 6 mm thickness
- Sources of ^{57}Co(122 keV) and ^{241}Am(60 keV)
- central collimation hole of 4 mm diameter
- V_{BIAS} = 75.52V,T=40°C

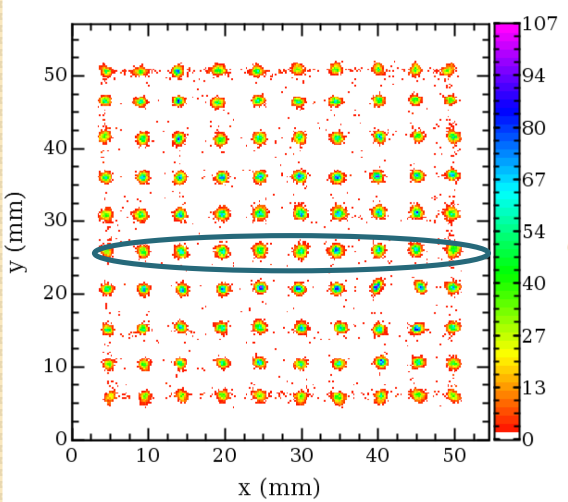

Reconstructed image of holes collimator

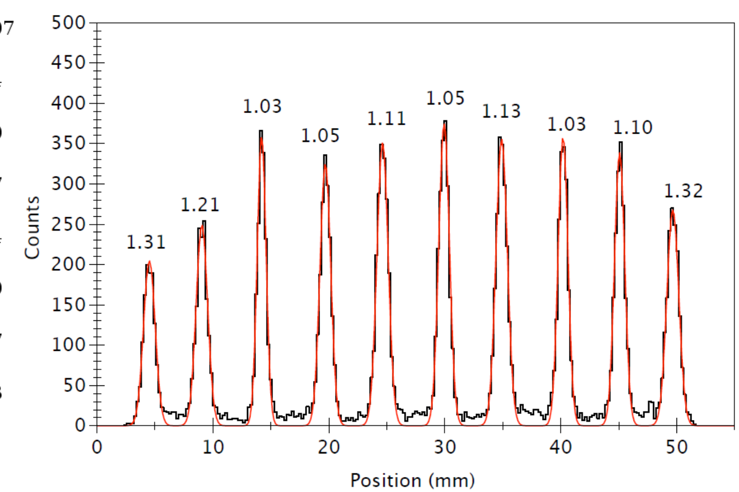

Spatial profile of 10 holes extracted from a line of the collimator

Spatial resolution:

- 1.13 mm @ 122 keV

Experimental conditions:

- $LaBr_3(Ce)$ – 6 mm thickness
- ^{57}Co(122 keV)
- 1 mm diameter of 10x10 spots spaced 5 mm apart
- V_{BIAS} = 75.52V,T=40°C
- Levenberg-Marquard reconstruction algorithm

SiPM applications

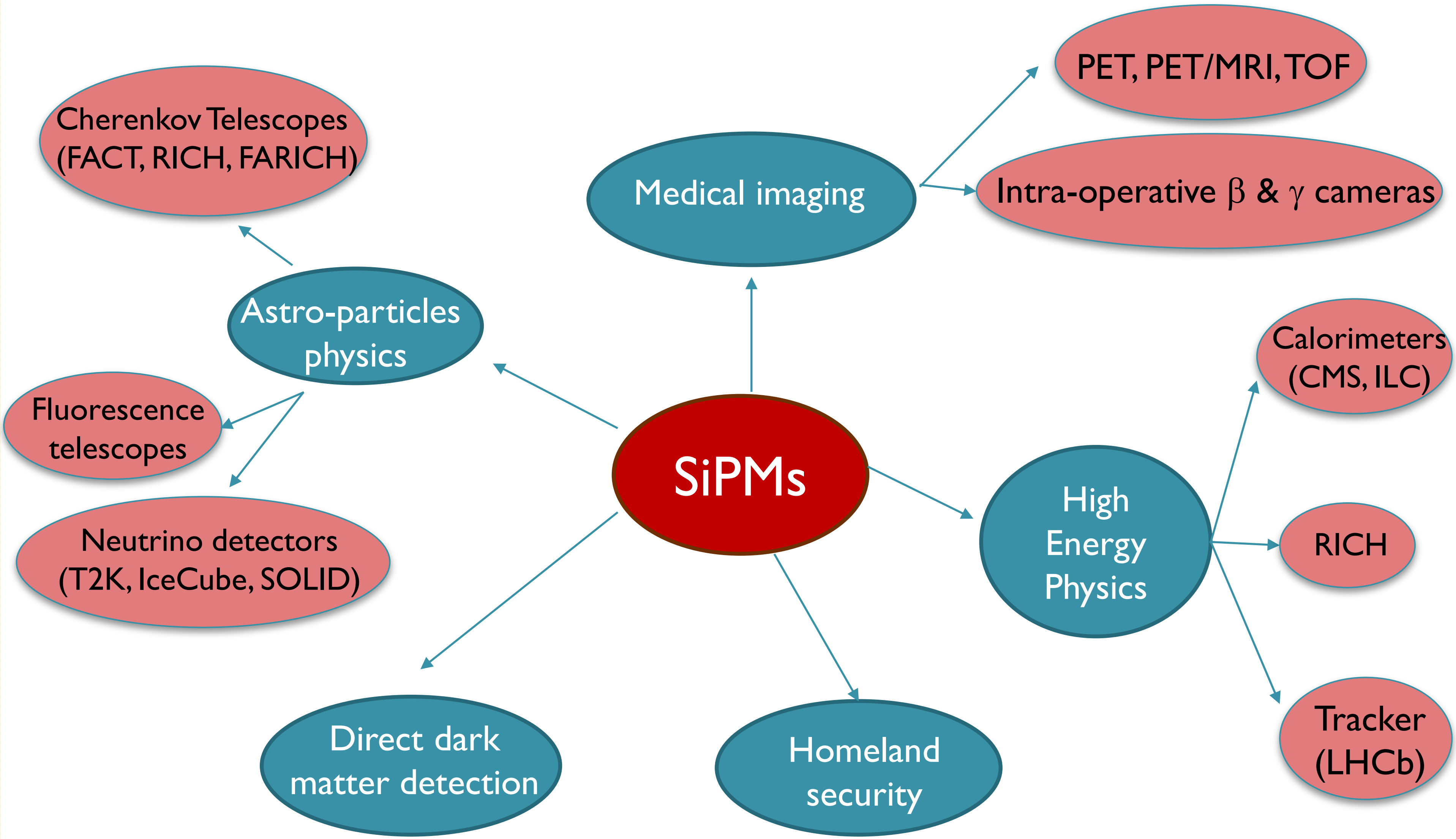

Discussion shifts from device features to how to select/implement them to dedicated application

….how to evaluate SiPM for various applications (1)

• Photon detection efficiency

- For many applications is the first parameter to review
- Is a function of wavelength
- It increases with the bias voltage and μcell size
  - consequences on peak values ⇒ very different from different vendors
- Points to consider:
  - Does the sensor have enough sensitivity at the required wavelength?
  - What overvoltage is needed to achieve the PDE and how does this impact on other performance parameters (DCR)?

• Signal shape (rise time, recovery time)

- SiPM rise time is very fast; however, the output signal is dominated by impedance of full array (~ns)
- Recovery time is given by the product of effective μcell capacitance and quenching resistor (O(10-100)ns)
  - Capacitance depends on area ⇒ recovery time vary for different μcell sizes
- Points to consider:
  - Is timing or count rate important for the application?
  - Careful study of the various sensor sizes and/or μcell sizes should be carried out

…..how to evaluate SiPM for various applications (2)

• Dark count rate

- Primary source of noise in a SiPM sensor
- Specially important for low light level applications or those with long integration times
- Standard devices today have
  - ~30-50 kHz/mm^2 @ 25°C
  - < 10 Hz/mm^2 @ -100°C
- It scales with μcell size (overall sensor size) and with overvoltage and temperature
  - It will impact on SNR
- Points to consider:
  - Is DCR quoted per mm^2 or for the whole sensor area?
  - Is DCR sufficiently low to achieve the required SNR for the application?
  - DCR values should be checked as a function of overvoltage and temperature
    - If higher temperatures are to be encountered, is the increase in DCR tolerable?
  - Evaluate how much afterpulses and cross-talk are important for the application
    - Trenches presence does not guarantee the best cross-talk (effective only for direct cross-talk suppression)

…..how to evaluate SiPM for various applications (3)

• Breakdown voltage and operating voltage

- Bias point at which the electrical field strength is sufficient to create a Geiger discharge
- Typical V_{BD} values at 25°C: HPK: ~50V; KETEK: ~ 24V; SensL: ~ 24.5V; FBK: ~ 28.5V
- It increases with increasing the temperature
  - Typical temperature coefficients: 20-55 mV/°C @ room temperature
  - Better stability at low T (bellow -100°C)
- Points to consider:
  - If multiple sensors have to be used in the system
    - Is the V_{BD} range enough narrow for the application? Are possibilities to adjust bias voltage /channel?
    - If a manufacture has agreed to provide sensors within a narrow V_{BD} range, is this from selecting the detectors, and if so has the selection increased the cost?
    - Has the impact of the power supply on the design and power requirements been considered?
    - Will temperature fluctuations in the application require a bias compensation circuit?

…..how to evaluate SiPM for various applications (4)

• Application specific performances

- Packaging
  - Structure in which the silicon chip is housed and has its terminals connected
  - Impact on how the sensor can be used
- Form factor
  - Size and shape and I/O type (pins or pads)
  - Points to consider:
    - Does it need to be compact to fit in a miniaturized system
    - Should the edge deadspace be minimized to allow for formation of a close-packed array?
    - Is there a preference for pins, which are generally hand soldered, or pads, which can be reflow soldered?
- Optical transmission
  - Clear material used to encapsulate the sensor can have impact on PDE
  - Glass on the TSV package offers advantages for UV wavelengths
  - Points to consider:
    - Does the application involve wavelengths that could be absorbed by the sensor encapsulated material?

…..some starting references

- SiPM physics and technology

- Basic level
  - N. Dinu, "Silicon Photomultiplier (SiPM)", Chapter 8

    Photodetectors – Material, Devices and Applications, Woodhead Publishing, Ed. B. Nabet, 2015
- Intermediate/detailed level
  - N. Dinu, "Instrumentation on Silicon detectors: from properties characterization to applications"

    Memoire d'habilitation à diriger des recherches, LAL-13-192, https://tel.archives-ouvertes.fr/tel-00872318/
- High level review
  - G. Collazuol, "Status and perspectives of Solid State Photo-Detectors", RICH 2013 workshop – Kanagawa
- Many, many articles on specific subjects…..
- Documentation on producers web pages:
  - http://www.hamamatsu.com/eu/en/4004.html
  - http://sensl.com/documentation/
  - http://advansid.com/resources

No. of papers in Google Scholar with the exact match of "silicon photomultiplier" in the title/abstract.body

Year	# papers
2000-2001	11
2002-2003	31
2004-2005	82
2006-2007	211
2008-2009	366
2010-2011	603
2012-2103	1117
2014- Nov. 2015	993

Additional slides

Analog vs digital SiPM – tight competition

Digital SiPM good features

- can turn off noisier micro-cells
- reduced after-pulsing (less charge)
- triggering at known photon level
- sophisticated triggering and time pickoff architecture
- inherently digital readout

Analog SiPM

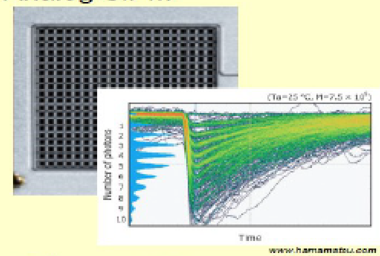

- Cells connected to common readout
- Analog sum of charge pulses
- Analog output signal

Digital SiPM

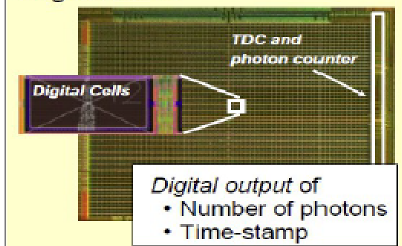

- Each diode is a digital switch
- Digital sum of detected photons
- Digital data output

In addition to Philips D-SiPM see other dSiPM by
→ Charbon et al at IEEE NSS 2013
→ Stoppa et al at IEEE NSS 2013

Digital SiPM most critical features

- scaled CMOS process has typically worse noise characteristics
  → mitigated by hottest single cells
- Fill Factor limited by area of silicon die used for digital circuits
  ... unless exploiting 3D technology → *see Tetrault, Fontaine et al at IEEE NSS 2013*
- lower PDE due also to lower QE → can be further optimized
- Additional radiation damages to integrated electronics → tests to be done

Active mode → “digital” SiPM

Philips Digital SiPM
APD cells & integrated electronics

- Cell area ~ 30x50μm^2
- Fill Factor ~ 50%

T.Frach at LIGHT 2011

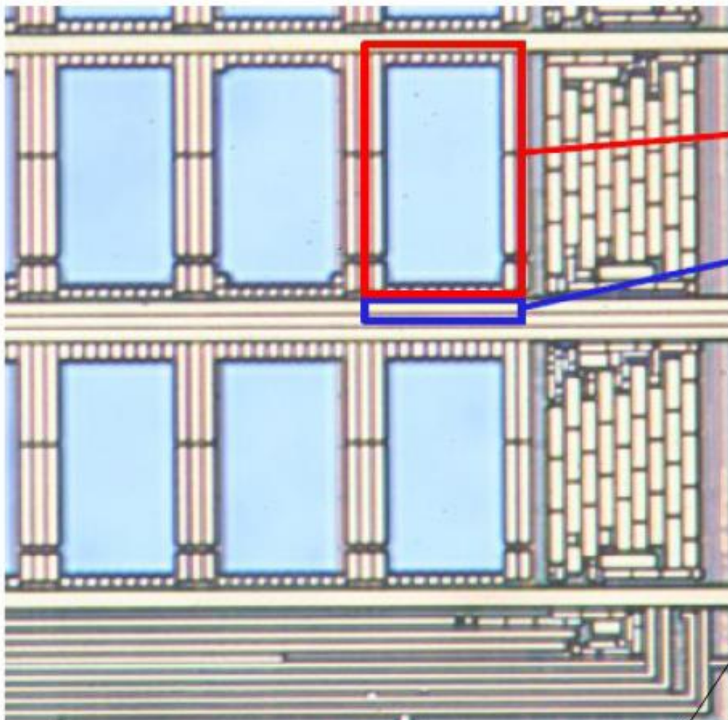

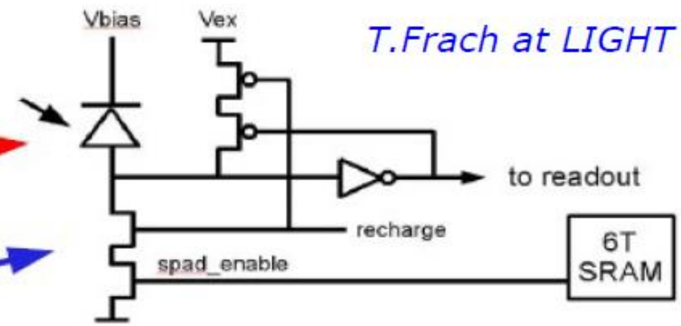

- Cell electronics area: 120µm²
- 25 transistors including 6T SRAM
- ~6% of total cell area
- Modified 0.18µm 5M CMOS
- Foundry: NXP Nijmegen

- reduced Fill Factor
- electronics exposed to radiation
→ additional radiation weakness

PDE vs T (constant ΔV=2V) - halogen lamp (CW)

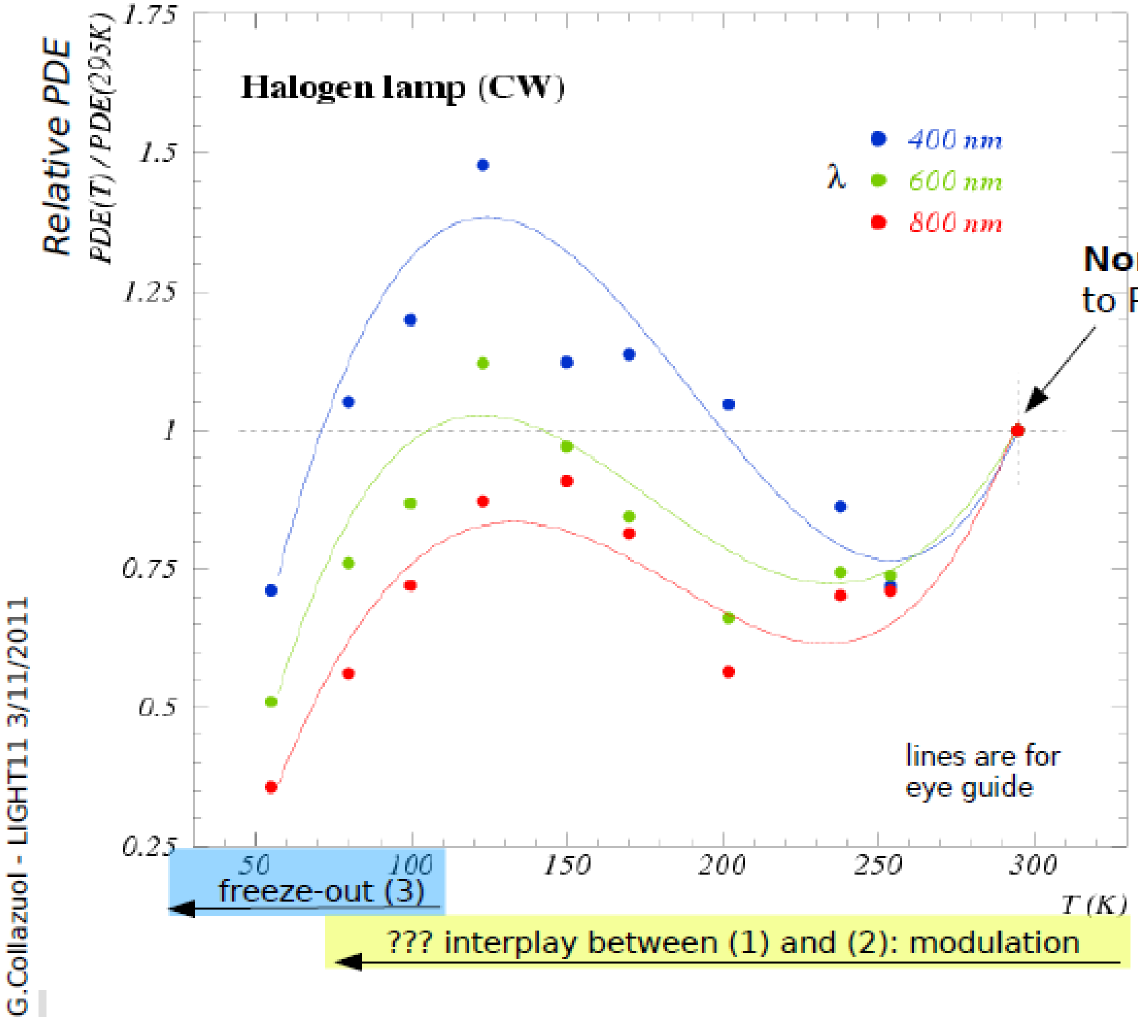

$PDE = I_{sipm} / G / I_{photons}$

Normalization to PDE(room T)

When T decreases we expect:

1) silicon E_{gap} increasing
→ longer attenuation length
→ lower QE (for longer λ)

2) mobility increasing
→ larger impact ionization
→ larger trigg. avalanche P_{01}

3) carriers freeze-out onset below 120K
→ loss of carriers

Radiation damage

- Radiation damage effects on SiPM:
  - increase of dark count rate due to introduction of generation centers
  - increase of after-pulse rate due to introduction of trapping centers
  - may change V_{BD}, leakage current, noise, PDE….

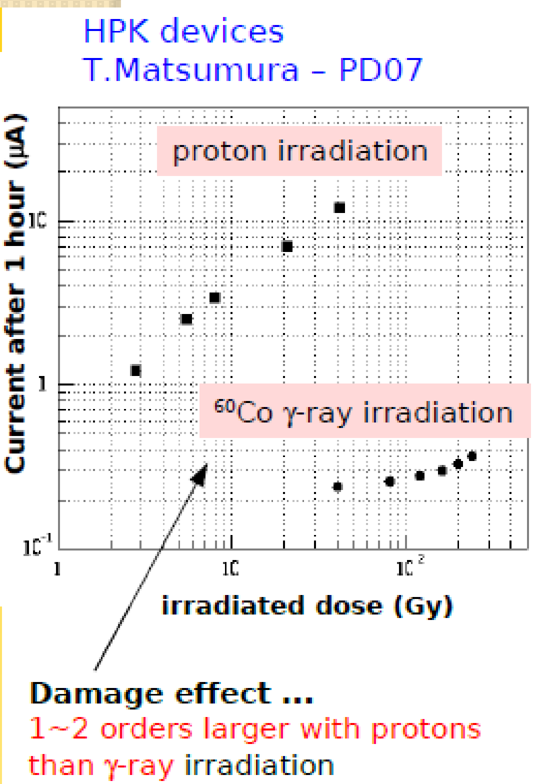

Damage effect …
almost the same for protons and neutrons

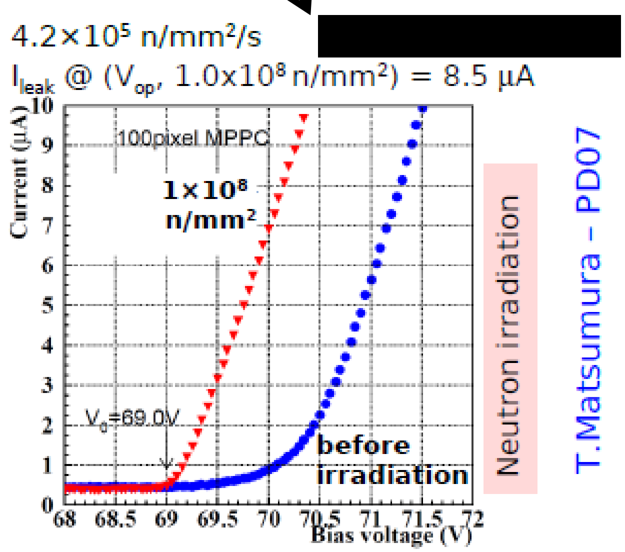

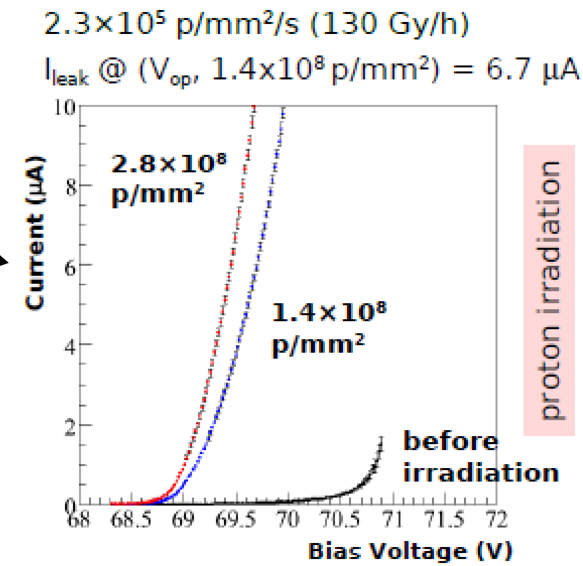

Read-out electronics of SIPMED

Board SIPMED2

Front side Back side

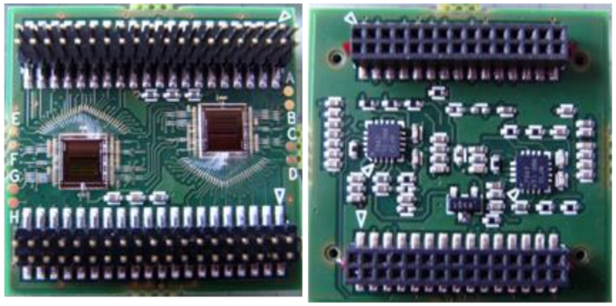

- 2 EASIROC chips/ elementary module
- two-channels externals ADC 12-bit, 2MSPS

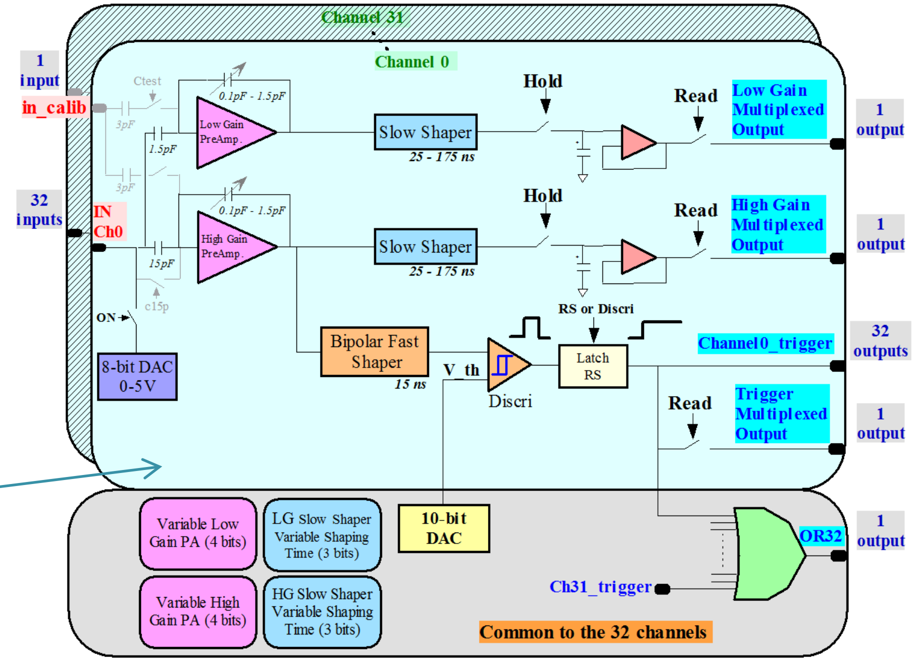

- **EASIROC chip**
  - 32 channels
  - 8-bit input DAC, 0-2.5V range
  - Low and high voltage pre-amplifiers, adjustable gain
  - charge measured at maximum amplitude of slow shapers (50 to 175 ns peaking time) by two Track and Hold blocks
  - fast trigger line, made of a fast shaper and a discriminator, provides the hold signal

Board SIPMED3

Front side Back side

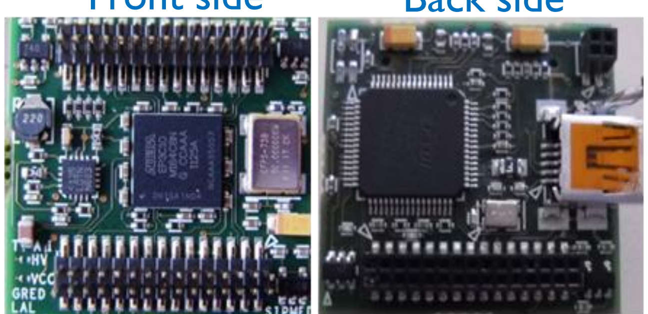

- ALTERA ciclone III FPGA
- FTDI FT2232H (USB protocol 2.0 Hi-speed, 440MBit/s)
- USB mini-connector for power supply and PC communication
- DC/DC converter for SiPM bias